Biophysical Journal Volume 72 June 1997 2524–2544

Two-Dimensional Components and Hidden Dependencies Provide Insight into Ion Channel Gating Mechanisms

Brad S. Rothberg, Ricardo A. Bello, and Karl L. Magleby
Department of Physiology and Biophysics, University of Miami School of Medicine, Miami, Florida 33101-6430 USA

ABSTRACT Correlations between the durations of adjacent open and shut intervals recorded from ion channels contain information about the underlying gating mechanism. This study presents an additional approach to extracting the correlation information. Detailed correlation information is obtained directly from single-channel data and quantified in a manner that can provide insight into the connections among the states underlying the gating. The information is obtained independently of any specific kinetic scheme, except for the general assumption of Markov gating. The durations of adjacent open and shut intervals are binned into two-dimensional (2-D) dwell-time distributions. The 2-D (joint) distributions are fitted with sums of 2-D exponential components to determine the number of 2-D components, their volumes, and their open and closed time constants. The dependency of each 2-D component is calculated by comparing its observed volume to the volume that would be expected if open and shut intervals paired independently. The estimated component dependencies are then used to suggest gating mechanisms and to provide a powerful means of examining whether proposed gating mechanisms have the correct connections among states. The sensitivity of the 2-D method can identify hidden components and dependencies that can go undetected by previous correlation methods.

INTRODUCTION

Ion channels are the gatekeepers that control the passive flux of ions through cell membranes (Hille, 1992). The gating of many ion channels has been described by assuming that the channels make transitions among a discrete number of open and closed states, with the rate constants for transitions among the states remaining constant in time for constant conditions (Horn and Lange, 1983; Aldrich et al., 1983; Sine et al., 1990; McManus and Magleby, 1991; Auerbach, 1993; Bezanilla et al., 1994; Zagotta et al., 1994; Colquhoun and Hawkes, 1995a). An estimate of the numbers of open and shut states in such discrete-state Markov models can be obtained by fitting sums of exponentials to the distributions of open and shut dwell times. The number of significant exponential components required to describe the distributions gives an estimate of the minimum number of open and shut states (Colquhoun and Hawkes, 1981, 1995a; Horn and Lange, 1983). It has proved more difficult to determine the connections among the various states because the potential number of different kinetic schemes, each with different connections, is large for most channels.

Full maximum likelihood fitting of the entire experimental record is perhaps the best method of identifying the most likely connections among states through the identification of the most likely kinetic scheme among those tested (Horn and Lange, 1983; Ball and Sansom, 1989; Chung et al., 1991; Fredkin and Rice, 1992; Qin et al., 1996; Colquhoun et al., 1996). Full likelihood methods inherently take the correlation information in the data into account during the fitting. However, this correlation information is available only in the context of predictions from the fitted kinetic scheme. Thus if the actual most likely scheme is not tested, then the most likely connections will not be found and the predicted correlation information may be in error. Furthermore, it can be difficult to evaluate whether the most likely of the examined schemes adequately describes the underlying gating process, because different gating mechanisms can predict identical one-dimensional dwell-time distributions and visually similar two-dimensional dwell-time distributions (Magleby and Weiss, 1990b).

To overcome some of these difficulties, a number of methods have been developed to examine correlations between sequential interval durations. These methods are typically based on an assumption of Markov gating, but are independent of any specific kinetic scheme. Both conditional dwell-time distributions and the correlation between the durations of each interval and that of the nth subsequent interval have been examined (Jackson et al., 1983; Fredkin et al., 1985; McManus et al., 1985; Colquhoun and Hawkes, 1987; Steinberg, 1987a; Ball et al., 1988; Blatz and Magleby, 1989). However, the conditional distributions and correlation data can be difficult to interpret because they present an average response, so that correlations of lesser magnitude or of opposite signs can be masked. Dependency plots have greatly improved the resolution of the correlation analysis (Magleby and Song, 1992), but are still limited by the fact that they present an average dependency, so that information about less dominant connections can be lost. Although the above techniques can be used to compare correlation information predicted by kinetic models to that obtained from the experimental data, the interpretation of any differences in correlation can be problematic, because it can be difficult to relate the average correlations predicted

Received for publication 16 December 1996 and in final form 13 March 1997.

The authors can be reached at the following E-mail addresses: B. S. Rothberg, bradr@chroma.med.miami.edu; R. A. Bello, rbello@chroma.med.miami.edu; K. L. Magleby, kmagleby@mednet.med.miami.edu.

0006-3495/97/06/2524/21 $2.00

by these techniques to the specific components predicted by kinetic models.

What is needed, then, is a method of extracting the specific correlation information about each underlying component directly from the experimental data, independently of a detailed kinetic scheme. This paper presents such a method, extending the studies of Fredkin et al. (1985), Steinberg (1987a), and Magleby and Song (1992). Two-dimensional (2-D) dwell-time distributions of adjacent open and closed interval durations are first fitted with sums of 2-D exponential components to determine the underlying 2-D components involved in the gating. The dependency of each 2-D component is then calculated from the observed volume of each component and the volume expected if open and shut intervals pair independently. The determined 2-D component dependencies give improved insight into the connections among states. They can suggest initial gating mechanisms and provide a powerful means of evaluating whether a given kinetic scheme has the correct connections among states. Finally, the resolution of the two-dimensional method allows hidden correlations to be detected that may be missed by some of the previous correlation methods. A preliminary report of some of these findings has appeared (Magleby et al., 1997).

METHODS

The first part of this study explores the possibility that information contained in the theoretical components underlying 2-D dwell-time distributions can give useful insight into gating mechanism. To do this, 2-D distributions and the theoretical 2-D exponential components underlying these distributions were calculated directly from examined kinetic schemes using the Q-matrix methods detailed in Fredkin et al. (1985) and Colquhoun and Hawkes (1995b). Calculations in the first part of the study were made assuming that the frequency response was infinite, equivalent to all intervals being detected. With this assumption of infinite frequency response, the Q-matrix methods gave exact solutions for the predicted distributions and the underlying components.

The second part of this study examines the possibility of determining the theoretical underlying 2-D components directly by fitting 2-D dwell-time distributions generated from single-channel data with sums of 2-D exponential components. To carry out this test, it is necessary to know the exact gating mechanism that generated the data. Because this is not known for experimental data, simulated single-channel data were analyzed.

The methods for simulating single-channel current, measuring interval durations using half-amplitude threshold detection for channel opening and closing, and log-binning the interval durations into dwell-time distributions have been described previously (Blatz and Magleby, 1986; Magleby and Weiss, 1990a,b). When binning to generate 2-D distributions, every open interval and its following shut interval and every shut interval and its following open interval were binned, with the logs of the open and shut times of each pair locating the bin on the x and y axes, respectively. Thus the number of interval pairs in the distribution was equal to the total number of intervals minus one. The maximum likelihood method for fitting 2-D distributions with sums (mixtures) of 2-D exponential components is detailed in the Appendix. The maximum likelihood methods for fitting 1-D distributions with sums (mixtures) of exponential components have been described previously (Colquhoun and Sigworth, 1995; McManus and Magleby, 1988).

The simulated single-channel current records were generated with various levels of time resolution, ranging from infinite time resolution (no filtering) to highly limited time resolution (heavy filtering). When single-channel data were simulated with limited time resolution, true filtering equivalent to a four-pole Bessel filter was used. With true filtering, detected intervals with true durations of less than about twice the dead time are narrowed (McManus et al., 1987; Magleby and Weiss, 1990a; Colquhoun and Sigworth, 1995). The measured durations of these intervals were corrected to their true durations before binning using the numerical method described in Colquhoun and Sigworth (1995). When single-channel data were simulated with filtering, noise equivalent to that typically present in single-channel records was also added. The standard deviation of the noise was equal to 15% of the single-channel current amplitude. The method used to simulate single-channel currents with true filtering and noise is detailed in Magleby and Weiss (1990a).

The ability to estimate the 2-D components by fitting sums of 2-D exponentials to 2-D distributions was assessed by comparing the fitted components to theoretical components. The theoretical components were calculated with Q-matrix methods (Fredkin et al., 1985; Colquhoun and Hawkes, 1995b) from the same scheme used to simulate the fitted data. Although Q-matrix methods give the exact descriptions of the theoretical distributions predicted by a kinetic scheme when the time resolution is infinite (no filtering), it is more problematic to calculate the theoretical values of the 2-D components that would be expected with true filtering and noise, as no analytical methods are available that take into account the full effects of true filtering and noise (Magleby and Weiss, 1990a). Therefore, an approximate method was used that assumes idealized filtering and no noise. This approximate method employed virtual states (Blatz and Magleby, 1986) and uncoupled kinetic schemes (Kienker, 1989) to account for missed events in the Q-matrix calculations, as developed by Crouzy and Sigworth (1990). For the few examples where the Crouzy and Sigworth (1990) method was used, the assumptions associated with this method would be expected to introduce a mean error of ~2% in the calculated rate constants (Magleby and Weiss, 1990a). An error of this magnitude would have a negligible effect on the results of the present study, as the predictions of the Crouzy and Sigworth method (1990) were used as an independent control for comparison purposes only, and were not involved in the fitting of 2-D dwell-time distributions with sums of exponential components.

For heavy levels of filtering, the missed intervals that result from filtering can introduce virtual components in the dwell-time distributions with time constants typically less than one-half the dead time (Roux and Sauve, 1985; Hawkes et al., 1992; Magleby and Weiss, 1990a). Most of the examples presented in this paper use no filtering, so that the virtual components would be not be present in these examples. For the examples with filtering, the fitting was typically started at twice the dead time (see Appendix), which excluded the detection of the virtual components. Because the virtual components were not detected in the fitting, they were excluded from the theoretical calculations when the theoretical calculations were used for comparison to the fitted components. The volumes of the theoretical components were then normalized to 1.0 after the exclusion.

Estimates of the expected variability in determinations of component dependency, when presented, were obtained by resampling with replacement (Efron, 1982; Horn, 1987; Press et al., 1992). The 2-D dwell-time distribution was first fitted to estimate the time constants and volumes of the 2-D components. The data in the 2-D distribution were then resampled by drawing adjacent open-shut interval pairs at random from the original distribution to form an artificial 2-D distribution containing the same number of interval pairs as the original distibution. The artificial distribution was then fitted with sums of 2-D components to estimate the time constants and volumes of the 2-D components. This process was repeated 200 times to obtain the distribution of the estimated values. The significance of apparent correlations was then determined with a nonparametric statistical test, as detailed in the Results.

The plots of dwell-time distributions and their underlying components are presented with log-binning (McManus et al., 1987; Magleby and Weiss, 1990b), using the Sigworth and Sine (1987) transformation that plots the square root of the numbers of observations per bin for constant bin widths on a log scale. Components underlying 2-D distributions can have negative numbers of interval pairs (negative volumes), which cannot be plotted directly with the Sigworth and Sine square root transformation. To allow

the plotting of bins with negative volumes, the plotted values per bin, $f_{plot}(t_o, t_c)$, were obtained from the calculated volumes with

$$f_{plot}(t_O, t_C) = \frac{f(t_O, t_C)}{|f(t_O, t_C)|} \sqrt{|f(t_O, t_C)|} \quad (1)$$

THEORY

For discrete state gating models in which the rate constants for transitions among the states remain constant in time (Markov gating), the one-dimensional (1-D) distributions of all open $f_o(t)$ and all closed $f_c(t)$ dwell times are described by the sums of exponential components, with the number of components given by the number of states:

$$f_O(t) = \sum_{i=1}^{N_O} \alpha_i \tau_i^{-1} \exp(-t/\tau_i) \quad (2)$$

$$f_C(t) = \sum_{j=1}^{N_C} \beta_j \tau_j^{-1} \exp(-t/\tau_j) \quad (3)$$

where N_O and N_C are the number of open and closed states, α_i and β_j are the areas, and τ_i and τ_j are the time constants of the components of the 1-D open and closed distributions, respectively (Colquhoun and Hawkes, 1981, 1995a). The areas of all open components in Eq. 2 and of all shut components in Eq. 3 each sum to unity.

The two-dimensional (2-D) distribution (joint density) of adjacent interval pairs described by each open dwell time and the following closed dwell time, $f_{OC}(t_O, t_C)$, is given by (Fredkin et al., 1985, from their equation 4.1)

$$f_{OC}(t_O, t_C) = \sum_{i=1}^{N_O} \sum_{j=1}^{N_C} V_{ij} \tau_i^{-1} \tau_j^{-1} \exp(-t_O/\tau_i) \exp(-t_C/\tau_j) \quad (4)$$

where N_O and N_C are the number of open and closed states, V_{ij} is the volume of each 2-D component (fraction of total open-closed interval pairs), t_O and t_C are the open and closed times, and τ_i and τ_j are the time constants of the open and closed exponential functions. The magnitude of each 2-D component (at zero time) is given by $V_{ij}\tau_i^{-1}\tau_j^{-1}$. The number of underlying 2-D components that sum to form the 2-D distribution is given by $N_O \times N_C$. The volumes of the $N_O \times N_C$ underlying components sum to 1.0. An expression similar to Eq. 4 gives the 2-D distribution of closed intervals followed by open intervals:

$$f_{CO}(t_C, t_O) = \sum_{i=1}^{N_C} \sum_{j=1}^{N_O} V_{ij} \tau_i^{-1} \tau_j^{-1} \exp(-t_C/\tau_i) \exp(-t_O/\tau_j) \quad (5)$$

If the data are consistent with microscopic reversibility, then $f_{oc}(t_o, t_c) = f_{co}(t_c, t_o)$ (Fredkin et al., 1985; Steinberg, 1987b; Song and Magleby, 1994), so that the open-closed and closed-open interval pairs can be combined into the same distribution, as is the case for the analysis of simulated data presented in this paper.

For discrete state Markov gating, the time constants that underlie the 2-D dwell-time distributions are identical to the time constants underlying the 1-D dwell-time distributions (Fredkin et al., 1985).

The maximum likelihood method of estimating the volumes and time constants of the individual 2-D components from 2-D dwell time distributions is given in the Appendix.

SIMPLIFICATION OF PRESENTATION AND TERMINOLOGY

The components describing the 1-D and 2-D dwell-time distributions in Eqs. 2–5 are conveniently referred to by their time constants, with one time constant (either open or shut) describing each 1-D component, and two time constants (one open and one shut) describing each 2-D component. Because the interval durations are exponentially distributed, the intervals in an exponential component range from brief to long, with the time constant indicating the mean duration of the intervals in that component. To simplify the writing, all open or shut intervals from a component will be referred to by the time constant of the component. For example, the phrase "long shut intervals" will be used to refer to all intervals in the 1-D exponential component of shut intervals with a long time constant. As another example, the phrase "brief open intervals adjacent to intermediate shut intervals" will be used to refer to all open-shut interval pairs in the 2-D component defined by an exponential distribution of open intervals with a brief time constant adjacent to an exponential distribution of shut intervals with an intermediate time constant.

The time constants of the various underlying components depend, in general, on one or more of the rate constants for the scheme, and often have no simple physical interpretation (Colquhoun and Hawkes, 1981, 1995a). Nevertheless, for some kinetic schemes that have been used to describe channel kinetics, the intervals in the various components can be assumed to arise mainly from transitions to specific states or groups of states (Colquhoun and Sakmann, 1985; Magleby and Song, 1992). Such schemes have been selected for analysis in this paper to simplify the presentation. Although such simplification places limitations on the interpretations, simplification is not necessary for the method presented here to be useful, as considered in the Discussion.

RESULTS PART 1: 2-D COMPONENTS CAN REVEAL USEFUL INFORMATION ABOUT GATING MECHANISM

The purpose of this section is to explore the possibility of using 2-D components and component dependencies to make predictions about potential gating mechanisms. Examples of 2-D components and component dependencies are presented and examined for various kinetic schemes to see how the information relates to connections among states. The components and dependencies in this section

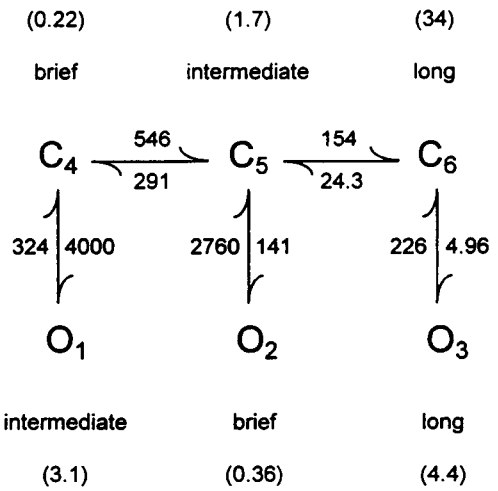

Scheme 1.

were calculated directly from the examined kinetic schemes.

The first hypothetical gating mechanism examined is described by Scheme 1, which has three open (O) and three closed (C) states. Scheme 1 also has three gateway states, given by the number of states that must be deleted to completely disconnect the open from the closed states (Fredkin et al., 1985; Colquhoun and Hawkes, 1995a). Calculations from the rate constants (units of s^{-1}) indicate that the open states have mean dwell times of 3.1, 0.36, and 4.4 ms, and the closed states have mean dwell times of 0.22, 1.7, and 34 ms, as shown.

1-D dwell-time distributions for Scheme 1

The (unconditional) distributions of all open and all closed intervals that would be generated by Scheme 1 are plotted separately in Fig. 1 as continuous lines using the Sigworth and Sine (1987) transformation that generates peaks at the time constants of the underlying components. Each distribution is described by the sum of three exponential components, as shown by the dashed lines in Fig. 1, suggesting a minimum of three open and three closed states, consistent with Scheme 1. The time constants and areas of the components calculated from Scheme 1 are listed in Table 1. The three open components O'_1, O'_2, and O'_3 arise directly from the open states O_1, O_2, O_3, respectively, because there are no direct connections between any of the open states. The brief shut component C'_4 (0.22 ms) arises mainly from sojourns to the closed state C_4, the intermediate shut component C'_5 (1.7 ms) arises mainly from sojourns to the compound closed state C_4-C_5, and the long shut component (45.0 ms) arises from sojourns to the compound closed state C_4-C_5-C_6.

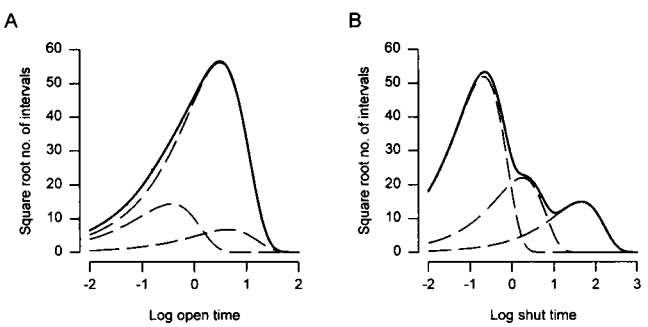

FIGURE 1 One-dimensional open (*A*) and shut (*B*) dwell-time distributions for Scheme 1 (——) and the underlying exponential components (– – –), which sum to form the distributions. The time constants and areas of the components are listed in Table 1. Units for time are log ms. The distributions are scaled using the Sigworth and Sine (1987) square root transformation for a hypothetical analysis of 100,000 open and shut intervals binned at a resolution of 25 bins per log unit.

Generation of the 2-D dwell-time distribution

For Scheme 1 with three open (N_O) and three closed (N_C) states, each open interval would be drawn from one of the three exponential components of open times in Fig. 1 *A* and Table 1, and each shut interval would be drawn from one of the three exponential components of shut times in Fig. 1 *B* and Table 1. Thus there are nine ($N_O \times N_C$) potential classes of open and shut interval pairs generated by Scheme 1, as indicated in Table 2 and by Eq. 4. Each of these nine classes would generate a 2-D component distribution of paired open and shut intervals with time constants given by the open and shut components from which the open and shut intervals were drawn (Eq. 4). The open and shut exponential functions that form a 2-D component would have equal magnitudes at time 0. The nine individual 2-D components would then sum to form the 2-D dwell-time distribution that would be observed experimentally when all pairs of open and shut intervals are binned into a 2-D distribution.

If the nine 2-D component distributions could be extracted from the experimentally observed 2-D dwell-time distribution, then it should be possible to gain insight into the potential connections among the states by comparing the observed volumes of each 2-D component distribution to the volumes expected for independent pairing of open and shut intervals (Magleby and Song, 1992). An excess of observed interval pairs would suggest that the open and closed states generating the interval pairs were more effectively connected than if there were a deficit. An absence of interval pairs would suggest that effective connections did not occur between the involved open and closed states.

Fig. 2 *A* presents the 2-D dwell-time distribution that would be observed for Scheme 1. The logarithm of the open and shut interval durations for each successive pair of intervals locates the bin for that pair on the x and y axes, respectively, and the z axis indicates the square root of the number of observed pairs in that bin (Magleby and Weiss, 1990b; Magleby and Song, 1992). The nine potential classes of open-closed interval pairs for Scheme 1 presented in Table 2 might be expected to generate up to nine peaks in

TABLE 1 Time constants and areas of the exponential components describing the 1-D open and closed dwell-time distributions for Schemes 1–4

	Scheme 1		Scheme 2		Scheme 3		Scheme 4	
Component	τ (ms)	Area	τ (ms)	Area	τ (ms)	Area	τ (ms)	Area
O'_1	3.086	0.9252	3.405	0.6040	3.542	0.4602	3.135	0.9038
O'_2	0.362	0.0612	0.343	0.0019	0.352	0.0278	0.358	0.0215
O'_3	4.425	0.0136	9.599	0.3941	5.432	0.5119	5.094	0.0747
C'_4	0.218	0.7914	0.217	0.8583	0.220	0.7439	0.218	0.7914
C'_5	1.807	0.1424	1.843	0.0949	1.706	0.1683	1.807	0.1424
C'_6	45.082	0.0662	54.545	0.0468	34.176	0.0879	45.082	0.0662

τ, Time constant.

Fig. 2 *A*, reflecting the nine underlying 2-D component distributions. Fewer than nine peaks are visible, however, suggesting that some of the classes may have insufficient pairs of intervals to be detected, or they may have overlapping time constants.

The nine 2-D component distributions are plotted in Fig. 3, and the open and closed time constants and volumes defining each of the 2-D component distributions are presented in Table 3. The time constants defining the 2-D components underlying the 2-D distribution (Table 3) are identical to those defining the 1-D components underlying the 1-D distribution (Table 1) (Fredkin et al., 1985; McManus and Magleby, 1989).

The volume of a 2-D component indicates the fraction of the total open-closed interval pairs that fall into that component. From Table 3 and Fig. 3 it can be seen that the volumes ranged from a high of 0.795 for component $O'_1C'_4$ to a low of -0.0038 for component $O'_2C'_4$. The volume of component $O'_3C'_5$ was also negative at -0.0005.

Theoretical considerations indicate that the 2-D components with negative volumes are associated with negative rate constants in an equivalent uncoupled kinetic scheme (Kienker, 1989; Crouzy and Sigworth, 1990). Although uncoupled schemes are highly useful for mathematical manipulation of the data, uncoupled schemes with negative rate constants would not have physical meaning. It will be shown in later sections that components with negative volumes indicate a lack of effective connections among the states associated with these components.

Calculation of the component dependency

To obtain a quantitative measure of the excess or deficit of interval pairs in each 2-D component over that expected if open and shut intervals paired independently (at random), the dependency (Magleby and Song, 1992) was calculated for each component. The first step was to calculate the expected volume of each 2-D component for independent pairing. Because the volumes of the individual 2-D components underlying the 2-D distributions sum to 1.0, they may be viewed as probabilities. Thus, for independent pairing of open and shut intervals, the probability of observing an open interval from open component O'_i adjacent to a shut interval from shut component C'_j is the product of the probabilities of observing the individual intervals separately:

$$V_{Ind}(O'_iC'_j) = \alpha_i \times \beta_j \quad (6)$$

where $V_{Ind}(O'_iC'_j)$ is the expected volume of the 2-D component $O'_iC'_j$ for independent pairing of open and shut intervals, and α_i and β_j are the areas of the 1-D open and shut components O'_i and C'_j, respectively.

The expected 2-D components for independent pairing are presented in Fig. 4, with the expected volumes indicated in Table 3 under V_{Ind}. Examination of Table 3 and Figs. 3 and 4 shows a clear difference between the volumes of the observed components and those expected for independent pairing. The actual component differences, $V_{Diff}(O'_iC'_j)$, were calculated from

$$V_{Diff}(O'_iC'_j) = V_{Obs}(O'_iC'_j) - V_{Ind}(O'_iC'_j) \quad (7)$$

where $V_{Obs}(O'_iC'_j)$ is the observed volume of each 2-D component, and $V_{Ind}(O'_iC'_j)$, as given by Eq. 6, is the expected volume if the open and shut intervals pair independently. The component differences are presented in Table 3 and Fig. 5, where it can be seen that four of the nine components had an excess of interval pairs, and five had a deficit. Component $O'_1C'_4$ had the greatest excess, with a surplus of 6.3% of the total number of interval pairs in all components, and component $O'_2C'_4$ had the greatest deficit, with a shortage of 5.2% of all interval pairs.

Although the component differences give a visual measure of the numbers of interval pairs in excess or deficit for each component, they do not indicate the fractional excess or deficit for each component, which can be especially useful for determining connections among states.

To determine the fractional excess or deficit of interval pairs for each component, the component dependency,

TABLE 2 The nine potential classes of open and shut interval pairs for a model with three open and three closed states

	C'_4	C'_5	C'_6
O'_1	$O'_1C'_4$	$O'_1C'_5$	$O'_1C'_6$
O'_2	$O'_2C'_4$	$O'_2C'_5$	$O'_2C'_6$
O'_3	$O'_3C'_4$	$O'_3C'_5$	$O'_3C'_6$

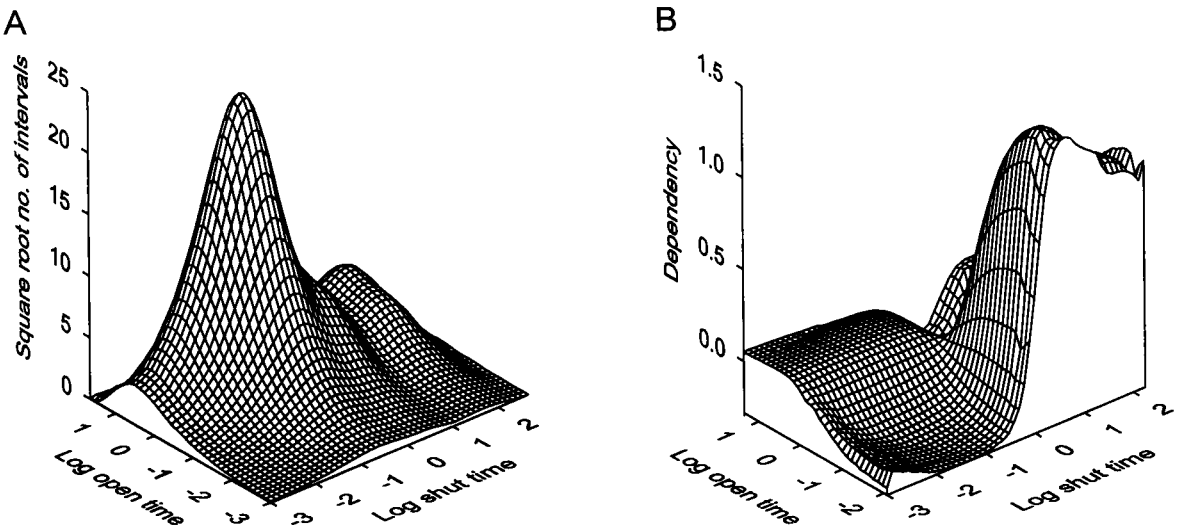

FIGURE 2 (*A*) Two-dimensional dwell-time distribution of adjacent open and shut intervals for Scheme 1. The log of the open and shut interval durations for each open-shut interval pair locates each bin on the *x* and *y* axes, respectively. Units for time are log ms. The distribution was scaled using the Sigworth and Sine (1987) square root transformation for a hypothetical analysis of 100,000 open and shut intervals. (*B*) The dependency plot calculated directly from the 2-D distribution in *A*, as described in Magleby and Song (1992). The data are plotted for binning at a resolution of 10 bins per log unit in this and Figs. 3–5. The surface plots were generated by the program SURFER (Golden Software, Golden, CO), using inverse distance interpolation.

cDep($O_i'C_j'$), was calculated with

$$\text{cDep}(O_i'C_j') = \frac{V_{\text{Obs}}(O_i'C_j') - V_{\text{Ind}}(O_i'C_j')}{V_{\text{Ind}}(O_i'C_j')} \qquad (8)$$

where $V_{\text{Obs}}(O_i'C_j')$ is the observed volume of each 2-D component, and $V_{\text{Ind}}(O_i'C_j')$ is the expected volume if the open and shut intervals pair independently.

Component dependencies of +0.5 or −0.5 would indicate a 50% excess or 50% deficit, respectively, of observed interval pairs when compared to that expected for independent pairing of open and shut intervals. A component dependency of −1.0 would indicate that no interval pairs were found in a component, and a component dependency less than −1.0 (supernegative) would indicate a component with negative volume. The calculated component dependencies for all nine components are presented in Table 3 and are plotted in Fig. 6 as a component dependency plot. The component dependencies ranged from −1.25 for component $O_3'C_5'$, indicating a negative volume, to 14.6 for component $O_3'C_6'$, indicating a 14.6-fold excess over that expected for independent pairing of intervals.

Interpretation of results for Scheme 1

Components with volumes less than or equal to 0, giving component dependencies less than or equal to −1.0

Three of the nine components, $O_2'C_4'$, $O_3'C_4'$, and $O_3'C_5'$, had observed volumes less than or equal to 0 (Table 3), suggesting that interval pairs from these three components did not occur for Scheme 1. This absence of interval pairs from these components is indicated by the essentially flat or negative observed distributions (Fig. 3) and component dependencies less than or equal to −1.0 (Table 3, Fig. 6). The absence of interval pairs from these three component distributions is even more striking when one considers that the individual unpaired open and shut intervals are present individually (Fig. 1 and Table 1), so that they would be expected to have detectable volumes if the pairing of intervals were independent (Fig. 4).

The absence of observed intervals for these three components is consistent with visual inspection of Scheme 1. Brief open intervals are unlikely to occur adjacent to brief shut intervals ($O_2'C_4'$), because the only connection from state O_2 to state C_4 is through the intermediate-duration closed state C_5. Long open intervals are unlikely to be adjacent to intermediate shut intervals, ($O_3'C_5'$), because the only connection from state O_3 to state C_5 is through the long closed state C_6, and long open intervals are unlikely to be adjacent to brief shut intervals ($O_3'C_4'$), because the only connection from state O_3 to state C_4 is through both the long closed state C_6 and the intermediate shut state C_5.

The above observations (together with further examples to be presented below) suggest that component dependencies less than or equal to −1.0 are typically associated with the situation in which the expected brief intervals cannot occur adjacent to specified intervals, because the only pathway between the states that generates the adjacent intervals involves transitions through compound states of considerably longer lifetimes.

Components with volumes greater than 0, giving component dependencies greater than −1.0

In contrast to the absence of interval pairs in components $O_2'C_4'$, $O_3'C_4'$, and $O_3'C_5'$, interval pairs from the remaining six

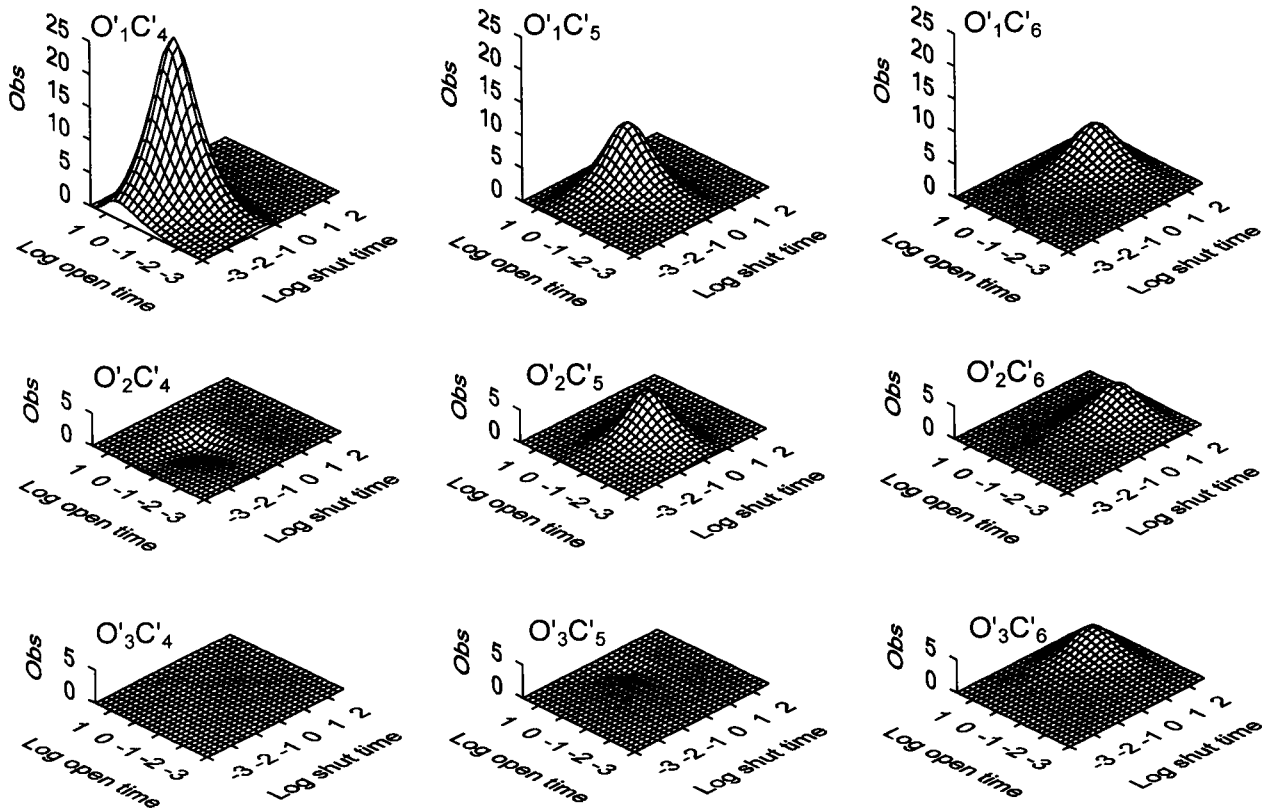

FIGURE 3 The nine 2-D components generated by Scheme 1. The intervals in these nine 2-D components sum to form the 2-D dwell-time distribution shown in Fig. 2 *A*. Calculating the 2-D components with Q-matrix methods from Scheme 1 or fitting the 2-D distribution in Fig. 2 *A* with sums of 2-D exponential components gave visually indistinguishable plots. The time constants and volumes of the 2-D components are listed in Table 3. The *z* axis, *Obs*, plots the square root of the number of interval pairs in each bin. Units for time are log ms.

components were observed (Table 3 and Fig. 3). Thus appropriate connections between open and closed states must exist for the six components with positive volumes, so that the relevant open and shut interval pairs can be adjacent to one another.

The brief open intervals are in greatest excess adjacent to intermediate shut intervals (cDep($O'_2C'_5$) = 4.35; Table 3 and Fig. 6), consistent with a direct connection of O_2 to one of the closed states in the compound shut state C_4-C_5. Brief open intervals are also in excess adjacent to long shut intervals (cDep($O'_2C'_6$) = 3.55), consistent with a direct connection of O_2 to one of the closed states in the compound shut state C_4-C_5-C_6. The supernegative component dependency of −1.08 for $O'_2C'_4$ suggests that O_2 does not connect directly to C_4. Thus O_2 would connect to C_5 or C_6. The greater dependency of $O'_2C'_5$ compared to $O'_2C'_6$ suggests that O_2 may connect to C_5 rather than to C_6.

TABLE 3 Kinetic 2-D components for Scheme 1

τ_{open} (ms)		τ_{shut} (ms)		V_{Obs}	V_{Ind}	V_{Diff}	cDep
O'_1	3.086	C'_4	0.218	0.7952	0.7322	0.0630	0.086
		C'_5	1.807	0.0963	0.1317	−0.0354	−0.269
		C'_6	45.082	0.0337	0.0613	−0.0276	−0.451
O'_2	0.362	C'_4	0.218	−0.0038	0.0484	−0.0522	−1.08
		C'_5	1.807	0.0466	0.0087	0.0379	4.35
		C'_6	45.082	0.0184	0.0041	0.0144	3.55
O'_3	4.425	C'_4	0.218	0.0000	0.0108	−0.0108	−1.00
		C'_5	1.807	−0.0005	0.0019	−0.0024	−1.25
		C'_6	45.082	0.0141	0.0009	0.0132	14.6

τ_{open}, open time constant; τ_{shut}, shut time constant; V_{Obs}, observed volume of 2-D component (determined by Q-matrix calculation); V_{Ind}, expected volume of 2-D component assuming independent (random) O-C pairings (Eq. 6); V_{Diff}, $V_{Obs} - V_{Ind}$ (Eq. 7); cDep, component dependency (Eq. 8).

Intermediate open intervals are in excess adjacent to brief shut intervals (cDep($O'_1C'_4$) = 0.086), and in deficit adjacent to intermediate (cDep($O'_1C'_5$) = −0.269) and long shut intervals (cDep($O'_1C'_6$) = −0.451), consistent with O_1 connecting to C_4 rather than to C_5 or C_6. The lesser deficit of $O'_1C'_5$ (−0.269) compared to that of $O'_1C'_6$ (−0.451) suggests that O_1 may be closer to C_5 than to C_6.

Long open intervals are in 14.6-fold excess adjacent to long shut intervals ($O'_3C'_6$), and do not occur adjacent to intermediate and brief shut intervals (cDep($O'_3C'_5$) = −1.25 and cDep($O'_3C'_4$) = −1.0), consistent with O_3 connecting directly to C_6.

The 14.6-fold excess of long open intervals adjacent to long shut intervals ($O'_3C'_6$) compared to the 3.55-fold excess of brief open intervals adjacent to long shut intervals ($O'_2C'_6$) is consistent with O_2 connecting to C_5 rather than to C_6, with the long shut intervals in $O'_2C'_6$ generated through the compound state C_4-C_5-C_6.

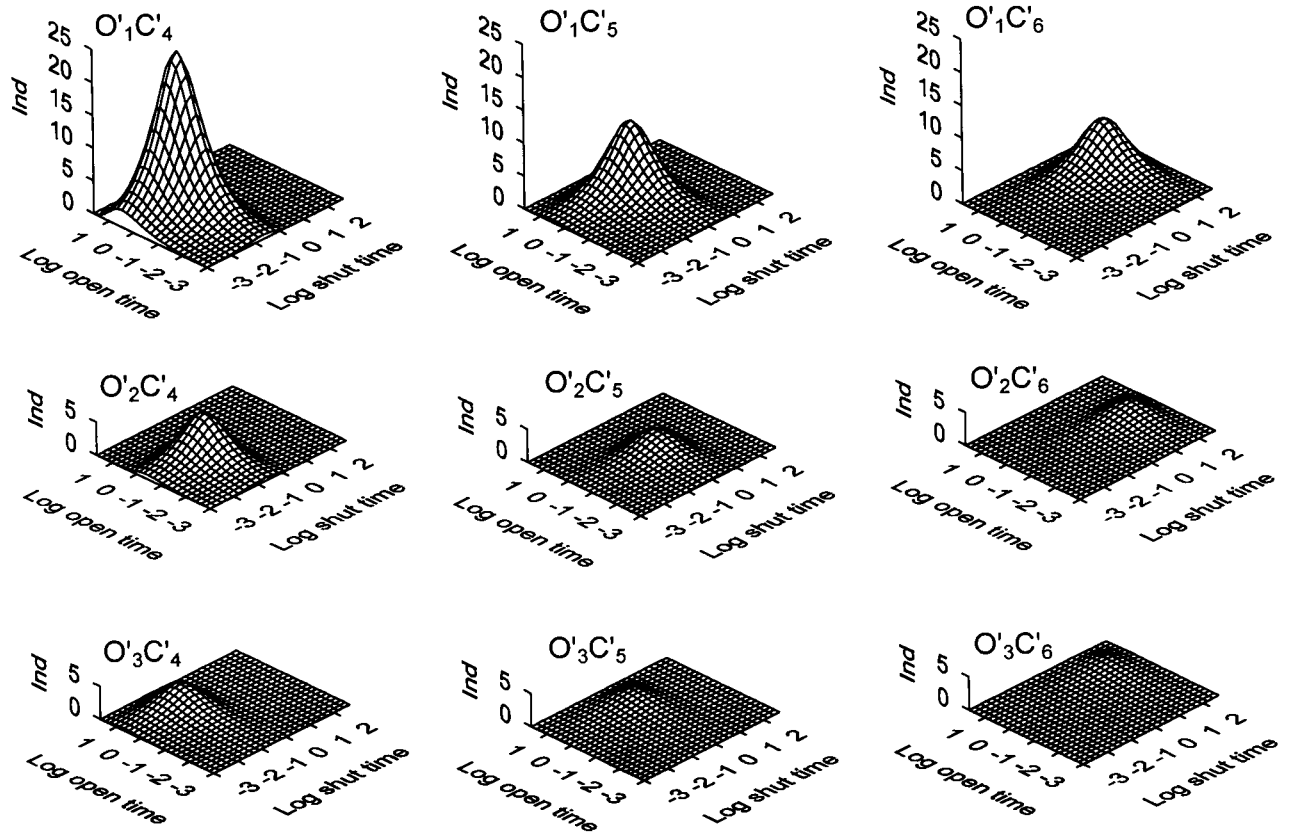

FIGURE 4 The nine hypothetical 2-D components that would be expected if the open and shut intervals in the 1-D components shown in Fig. 1 and Table 1 for Scheme 1 paired independently. The *z* axis, *Ind*, plots the square root of the number of interval pairs in each bin. Units for time are log ms.

From this discussion it can be seen that component dependencies can suggest useful information about possible connections among states.

Revealing hidden dependencies

In the above sections, the 2-D dwell-time distribution was separated into underlying 2-D components to determine the dependency of each component. An average measure of dependency can be obtained directly from 2-D dwell-time distributions without separating the data into components (details in Magleby and Song, 1992). Fig. 2 *B* presents such a plot of average dependency for the distribution in Fig. 2 *A* for Scheme 1, where the fractional excess or deficit of interval pairs for each bin over that expected for independent pairing of intervals is plotted. Information about five of the expected nine components is apparent in Fig. 2 *B*, with three peaks indicating an excess of intervals and two depressions indicating a deficit of intervals.

Because Scheme 1 would generate nine components, information about four of the components is apparently hidden in Fig. 2 because of the averaging that occurs when dependency is calculated from the 2-D distribution rather than from the underlying components. For example, Table 3 and Figs. 5 and 6 show that there is a deficit of long open intervals adjacent to brief closed intervals ($O'_3C'_4$). The dependency arising from this deficit of intervals is hidden in Fig. 2 *B* because of the excess of intermediate open intervals adjacent to brief closed intervals ($O'_1C'_4$). Thus analysis of component dependencies rather than average dependencies obtained directly from distributions provides a means of obtaining information about potentially hidden dependencies. Such information can give critical insight into the connections among states.

Component dependencies for additional models

The above sections examined a single kinetic scheme in detail, showing the various steps required to obtain the component dependencies and the interpretation of the results. The following section examines additional kinetic models to further examine the relationship between component dependencies and gating mechanisms.

Single transition pathway between open and closed states

Scheme 2 is similar to Scheme 1, except that the open states are connected to form a compound state and there is only one connection between the open and shut states, giving a single gateway state. The rate constants were selected so that the lifetimes of the individual states were identical to those in Scheme 1.

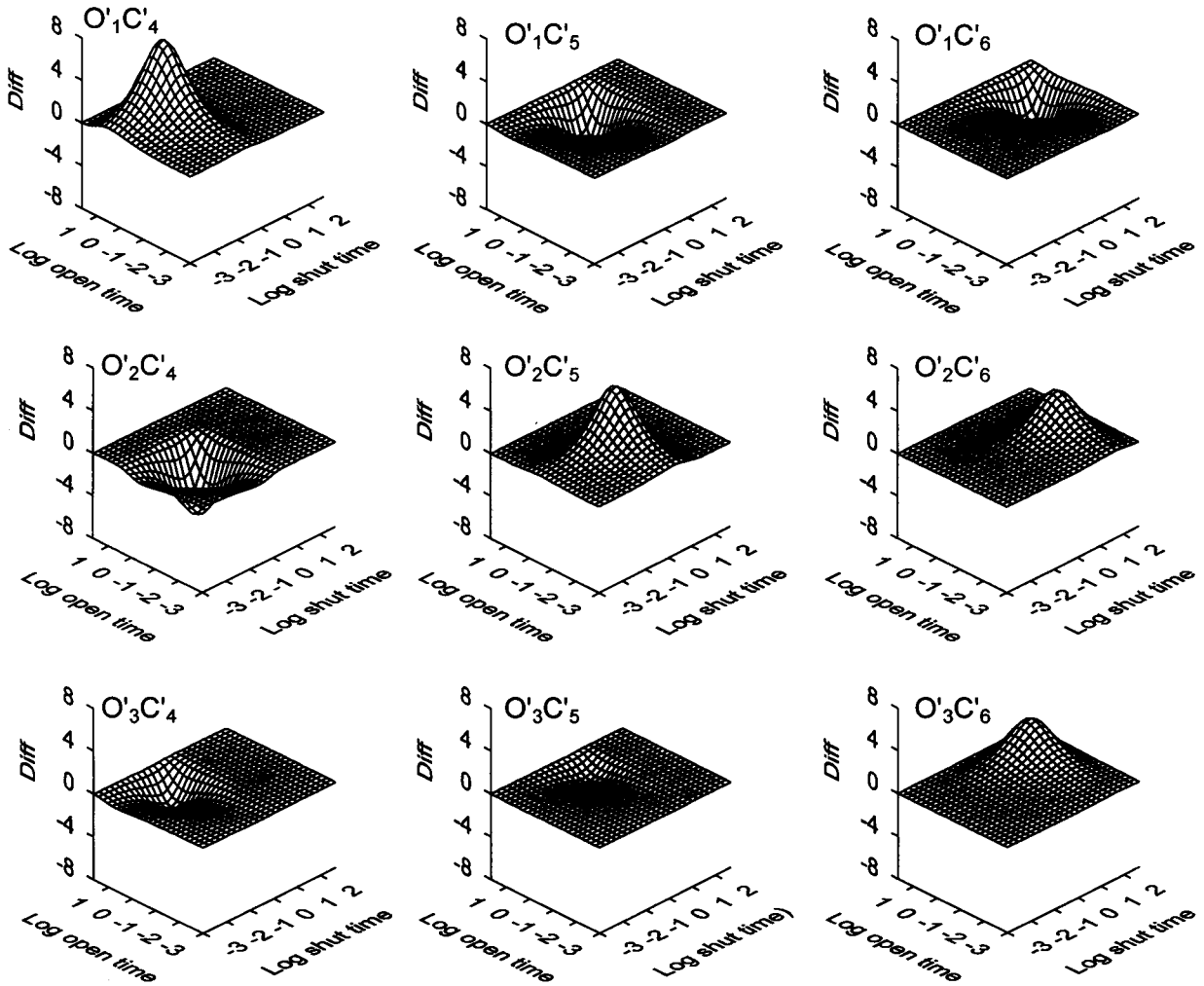

FIGURE 5 Plots of the differences, *Diff*, between the observed number of intervals in each bin in Fig. 3 and the expected number for independent pairing in Fig. 4. Positive or negative component differences indicate that there is an excess or deficit of intervals, respectively, over that expected if intervals paired independently. Units for time are log ms.

With three open and three closed states for Scheme 2, the 1-D distributions of open and shut intervals were each described by the sum of three exponential components, as shown in Table 1. For this scheme the intermediate open component O_1' results mainly from sojourns to O_1, and the long open component O_3' results mainly from sojourns to the compound open state O_1-O_2-O_3. Because the brief open state O_2 can only be reached indirectly through the intermediate open state O_1, there is a very limited area of 0.0019 in the brief open component O_2'.

For Scheme 2, all of the transitions between open and closed states must pass through the single transition pathway -O_1-C_4-. The consequence of this is that adjacent intervals pair independently, giving component dependencies of zero. This is shown in Table 4, where the observed volumes and volumes expected for independent pairing of intervals are identical. Thus an observation that all of the component dependencies are zero would suggest a single gateway state.

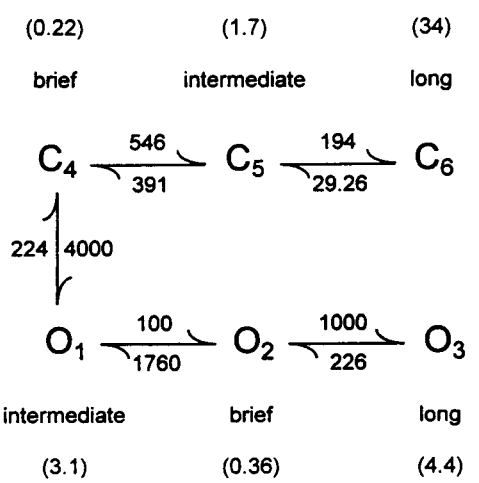

Scheme 2.

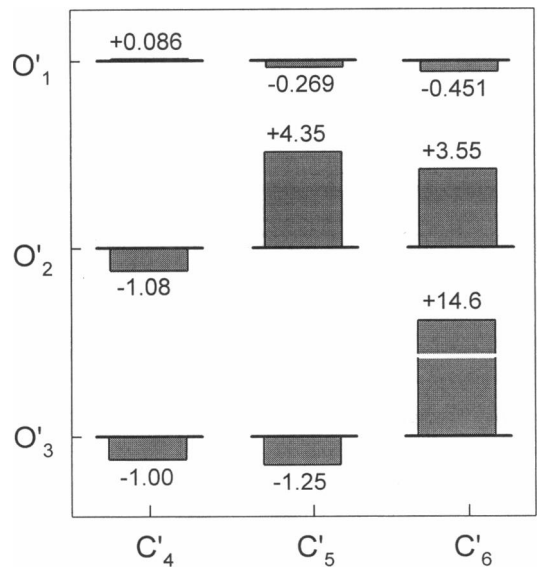

FIGURE 6 Component dependency plot for Scheme 1. The bars plot the component dependencies from Table 3, and the numbers indicate their values.

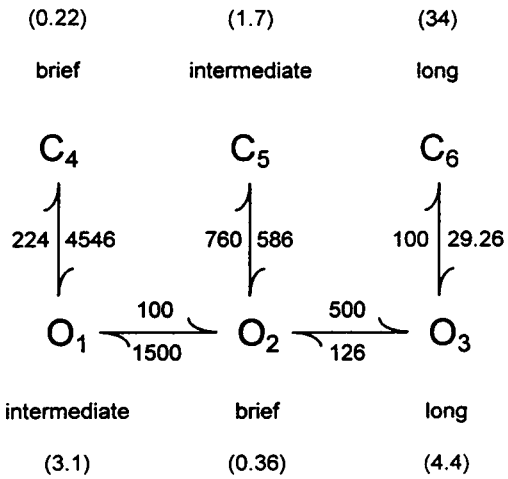

Scheme 3.

Compound open states

Scheme 3 is similar to Scheme 1, except that the open states are now connected to form a compound open state and the closed states are isolated without transition pathways among them. The rate constants were selected so that the individual lifetimes of the states were identical to those in Scheme 1. With three open and three closed states, the 1-D distributions of open and shut intervals were each described by the sums of three exponential components, as shown in Table 1.

The three shut components C'_4, C'_5 and C'_6 arise directly from the three closed states C_4, C_5, and C_6, respectively, because of the lack of direct connections between closed states. The intermediate open component O'_1 arises mainly from transitions to the compound open state O_1-O_2, the brief open component O'_2 arises mainly from transitions to the open state O_2, and the long open component O'_3 arises from transitions to the compound open state O_1-O_2-O_3. Table 5 presents the component volumes and dependencies for Scheme 3, and Fig. 7 presents the component dependency plot.

TABLE 4 Kinetic 2-D components for Scheme 2

τ_{open} (ms)		τ_{shut} (ms)		V_{Obs}	V_{Ind}	V_{Diff}	cDep
O'_1	3.405	C'_4	0.217	0.5184	0.5184	0.0000	0.000
		C'_5	1.843	0.0573	0.0573	0.0000	0.000
		C'_6	54.545	0.0283	0.0283	0.0000	0.000
O'_2	0.343	C'_4	0.217	0.0016	0.0016	0.0000	0.000
		C'_5	1.843	0.0002	0.0002	0.0000	0.000
		C'_6	54.545	0.0001	0.0001	0.0000	0.000
O'_3	9.599	C'_4	0.217	0.3383	0.3383	0.0000	0.000
		C'_5	1.843	0.0374	0.0374	0.0000	0.000
		C'_6	54.545	0.0184	0.0184	0.0000	0.000

There are a number of important differences in the connectivity information for Scheme 3 when compared to Scheme 1 (compare Table 5 to Table 3 and Fig. 7 to Fig. 6). This section examines four of the key differences that place major restrictions on the connections among the states, focusing on whether the component dependencies for a given component are greater or less than -1.0.

The first important difference between Scheme 3 and Scheme 1 is the supernegative component dependency of -2.28 for component $O'_1C'_6$ in Scheme 3 compared to -0.451 for the same component in Scheme 1. A supernegative component dependency of -2.28 suggests a kinetic scheme in which intermediate open intervals O'_1 cannot be adjacent to long shut intervals C'_6. Such pairing does not occur for Scheme 3, because transitions from O_1, the state that mainly generates the intermediate open component O'_1, must first pass through O_2 and O_3 (generating a long open interval) on the path to the long closed state C_6.

The second major difference between Schemes 3 and 1 is the supernegative component dependency of -1.36 for component $O'_2C'_6$ in Scheme 3 compared to the positive component dependency of 3.55 for this same component in Scheme 1. The supernegative component dependency suggests a kinetic scheme in which brief open intervals O'_2 cannot be adjacent to long shut intervals C'_6. Such pairing does not occur for Scheme 3 because transitions from O_2, the state that mainly generates the brief open component O'_2, must first pass through O_3, generating a long open interval on the path to the long closed state C_6.

The third and fourth major differences between Schemes 3 and 1 are the component dependencies of -0.259 and 0.037 for $O'_3C'_4$ and $O'_3C'_5$, respectively, for Scheme 3 compared to the supernegative component dependencies for both of these components for Scheme 1. The compound open state O_1-O_2-O_3 in Scheme 3, which generates the long open intervals O'_3, provides connections for long open intervals to be adjacent to intermediate and brief shut intervals for Scheme 3. These connections do not exist in Scheme 1.

TABLE 5 Kinetic 2-D components for Scheme 3

τ_{open} (ms)		τ_{shut} (ms)		V_{Obs}	V_{Ind}	V_{Diff}	cDep
O'_1	3.542	C'_4	0.220	0.4677	0.3424	0.1253	0.366
		C'_5	1.706	0.0441	0.0774	−0.0333	−0.430
		C'_6	34.176	−0.0516	0.0404	−0.0920	−2.28
O'_2	0.352	C'_4	0.220	−0.0061	0.0207	−0.0268	−1.30
		C'_5	1.706	0.0348	0.0047	0.0301	6.43
		C'_6	34.176	−0.0009	0.0024	−0.0033	−1.36
O'_3	5.432	C'_4	0.220	0.2823	0.3808	−0.0985	−0.259
		C'_5	1.706	0.0893	0.0861	0.0032	0.037
		C'_6	34.176	0.1403	0.0450	0.0953	2.12

Open and shut states connected in loops

Scheme 4 is similar to Schemes 1–3, except that transitions between open and shut states can occur in loops due to additional transition pathways. The rate constants were selected for Scheme 4 so that the lifetimes of the individual states were identical to those in Scheme 1 while maintaining microscopic reversibility (Colquhoun and Hawkes, 1995a). With three open and three closed states, the 1-D distributions of open and shut intervals were each described by the sums of three exponential components, as shown in Table 1. The effects of adding the additional transition pathways can be seen by comparing the results in Table 6 and Fig. 8 for Scheme 4 to those in Tables 3–5 and Figs. 6 and 7 for Schemes 1–3. Only two of the differences will be discussed. For Scheme 1, long open intervals do not occur adjacent to either intermediate shut intervals (cDep($O'_3C'_5$) = −1.25) or brief shut intervals (cDep($O'_3C'_4$) = −1.00) because the only pathway from open state O_3 to the closed states C_5 and C_4 is through the longer closed state C_6 (Table 3 and Fig. 6). In Scheme 4, the added transition pathways between the open states O_1, O_2, and O_3 provide a pathway from the long open state O_3 through the briefer duration open states to the

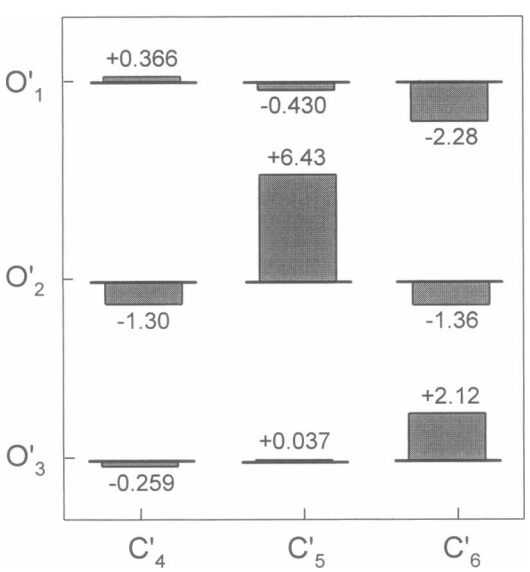

FIGURE 7 Component dependency plot for Scheme 3. The 2-D components are detailed in Table 5.

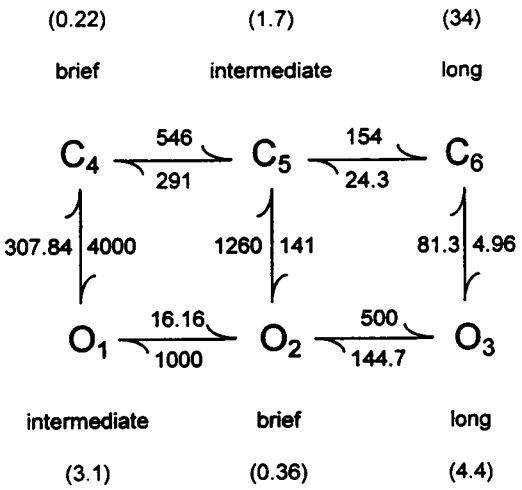

Scheme 4.

intermediate and brief closed states, allowing long open intervals to occur adjacent to intermediate and brief shut intervals, with component dependencies of 0.619 and −0.500, respectively (Table 6 and Fig. 8).

RESULTS PART 2: EXTRACTING THE 2-D COMPONENTS AND DEPENDENCIES FROM 2-D DWELL-TIME DISTRIBUTIONS

The time constants and the volumes of the 2-D components presented in the figures and tables in the above sections were calculated from the kinetic schemes using numerical techniques (see Methods). This approach is not available for experimental data, as the kinetic scheme is not known. Therefore this section explores the feasibility of estimating the underlying 2-D components directly from the 2-D dwell-time distributions. The fitting of the 2-D components requires an assumption of Markov gating, but is independent of any specific kinetic scheme. The fitted parameters are the time constants and volumes describing the 2-D components. The goal of this analysis is to extract the useful correlation information in the form of component dependencies to suggest possible gating mechanisms. The extracted component dependencies can also be used to determine whether the most likely models found by various

TABLE 6 Kinetic 2-D components for Scheme 4

τ_{open} (ms)		τ_{shut} (ms)		V_{Obs}	V_{Ind}	V_{Diff}	cDep
O'_1	3.135	C'_4	0.218	0.7654	0.7152	0.0502	0.070
		C'_5	1.807	0.1070	0.1287	−0.0217	−0.169
		C'_6	45.082	0.0314	0.0599	−0.0285	−0.476
O'_2	0.358	C'_4	0.218	−0.0036	0.0170	−0.0206	−1.21
		C'_5	1.807	0.0182	0.0031	0.0151	4.94
		C'_6	45.082	0.0069	0.0014	0.0055	3.84
O'_3	5.094	C'_4	0.218	0.0296	0.0591	−0.0295	−0.500
		C'_5	1.807	0.0172	0.0106	0.0066	0.619
		C'_6	45.082	0.0279	0.0049	0.0230	4.65

fitting procedures account for the correlation information in the data (see Discussion).

Single-channel current records were simulated for various kinetic schemes (see Methods), binned into 1-D and 2-D dwell-time distributions (examples in Figs. 1 and 2), and fitted with sums of 1-D and 2-D exponential components, respectively, using maximum likelihood methods. The 1-D fitting methods have been described previously (Colquhoun and Sigworth, 1985; McManus and Magleby, 1988). The 2-D fitting methods are described in the Appendix.

Estimating the time constants and volumes of the 2-D components by likelihood fitting

The first question examined was whether the underlying 2-D components could be determined from ideal data with no filtering or noise and with large numbers of events to reduce stochastic variation to insignificant levels. A total of 2,000,000 open and shut intervals were simulated for Scheme 1, binned into a 2-D distribution, and fitted with sums of 2-D exponential components to estimate the number of significant 2-D components (Eqs. 4 and A6). The fitting was started with a single open and a single shut time constant, giving a single 2-D component, as would be the case for a model with one open and one closed state. The fitting was then repeated with up to four open and four shut time constants to give a total of up to 16 2-D components, as would be the case for a model with four open and four closed states. The log-likelihood values for the fits were entered into Table 7. The number of significant 2-D components was then determined by applying the likelihood ratio test, taking into account the difference in the numbers of free parameters (see Eq. A8 and Tables 9 and 10 in the Appendix).

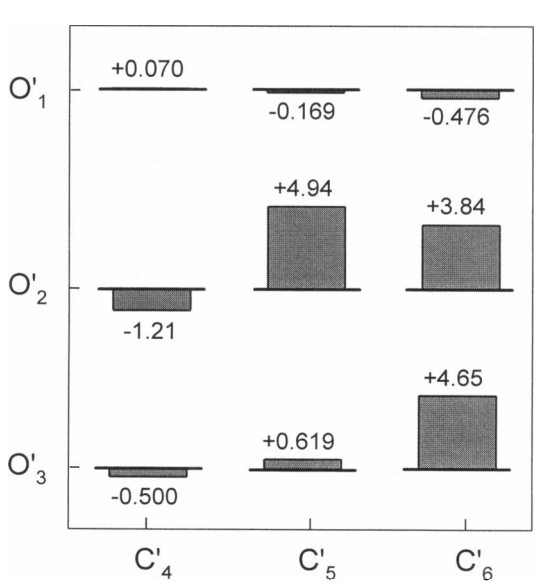

FIGURE 8 Component dependency plot for Scheme 4. The 2-D components are detailed in Table 6.

Fitting with three open and three closed time constants, giving nine 2-D components, was significantly better ($p \ll 0.001$) for Scheme 1 than fitting with two open and three closed time constants or three open and two closed time constants. Fitting with more than three open and three closed time constants did not improve the likelihood significantly. Thus the correct number of time constants was determined by 2-D likelihood fitting. Decreasing the total number of open and shut intervals to 200,000 or to 50,000 still gave the correct number of significant open and shut time constants ($p < 0.001$ and $p < 0.01$, respectively). Decreasing the total number of open and shut intervals further to 20,000 resulted in the detection of all three shut time constants, but only two of the three open time constants.

The ability of likelihood fitting to detect the nine 2-D components for Scheme 1 with 50,000 intervals shows the power of this technique, considering that the rate constants in Scheme 1 were selected to place a severe test on fitting techniques. The time constant of the intermediate open component was only 30% less than the time constant of the long open component, and the summed volume of the three 2-D components associated with the long open component was only 1.36% of the total volume of all nine components (Table 3). On this basis, it is perhaps not surprising that the long open component was not detected with a total of 20,000 open and shut intervals, as there would be a total of only about 136 open intervals from this component.

The estimates of the time constants and the volumes of the nine significant 2-D components determined by fitting 2,000,000 open and shut intervals with sums of 2-D exponentials are not presented, as they were essentially the same as the theoretical values in Table 3. For this simulated data set, the three open and three closed time constants that define the nine 2-D components in Table 2 were estimated to be within 0.5% of the theoretical values, and the volumes of the six components with volumes greater than 1% were estimated to be within 2% of the theoretical values. For the components with volumes less than 1%, the percentage differences were typically larger, but would have little effect on the useful information about the connections. For example, the component of brief open intervals adjacent to brief shut intervals ($O'_2C'_3$) had a theoretical volume of -0.0038 and a fitted volume of -0.0029, and the component of long open intervals adjacent to intermediate shut intervals ($O'_3C'_5$) had a theoretical volume of -0.0005 and a fitted volume of -0.001. Thus the components whose volumes were found to be negative by theoretical calculations from the kinetic schemes in the previous section were also found to be negative with practical fitting of the 2-D dwell-time distribution.

2-D fitting can detect hidden 1-D components

Interestingly, fitting the 1,000,000 open intervals for Scheme 1 with sums of 1-D exponentials resulted in the detection of only two significant open components, instead

TABLE 7 Log-likelihood values of the distributions described by Eq. 4 with the indicated number of open and closed time constants, for simulated adjacent open and shut intervals from Scheme 1

No. of shut time constants	No. of open time constants			
	1	2	3	4
1	−16,399,638.0	−16,390,209.7	−16,390,209.7	−16,390,209.7
2	−13,183,547.7	−13,154,418.1	−13,154,098.5	−13,154,098.3
3	−13,075,458.5	−13,041,005.7	−13,040,556.8*	−13,040,556.8
4	−13,075,458.5	−13,041,001.8	−13,040,556.7	−13,040,553.8

*$p < 0.001$.

The likelihood ratio test (Eq. A8) indicated three significant open time constants and three significant shut time constants underlying the most likely 2-D dwell-time distribution (Eq. 4). All adjacent open-shut and all adjacent shut-open pairs of intervals from 2×10^6 simulated intervals were used in the fitting.

of the three that could be detected with 2-D fitting of only 50,000 open and shut intervals. Such 1-D fitting of open intervals is equivalent to 2-D fitting with a single shut time constant. It can be seen from the top row of Table 7 that fitting with three or four open time constants and one shut time constant did not increase the log-likelihood over that obtained for fitting with only two open time constants and one shut time constant. When fitting with one shut time constant, where all of the open intervals would be contained in a single 1-D plane, the 13,600 intervals ($10^6 \times 0.0136$) in the long open component O_3' (Table 1, Scheme 1) were too few to be detected compared to the 925,200 intervals ($10^6 \times 0.9252$) in the intermediate open component O_1', because of their similar time constants.

With 2-D fitting, the long and intermediate open intervals were effectively separated into different 1-D planes because essentially all of the 13,600 long open intervals were adjacent to long shut intervals, $O_3'C_6'$, whereas only 33,700 of the 925,200 intermediate open intervals were adjacent to long shut intervals, $O_1'C_6'$ (Table 3). The exclusion of over 96% of the intermediate open intervals from the conditional distribution of long open intervals with 2-D fitting allowed the long open intervals to be detected with more than 40-fold increased sensitivity over 1-D fitting in this example.

One million open and shut intervals were simulated without filtering, binned into a 2-D dwell-time distribution, and fitted with sums of 2-D exponential components. As expected from the scheme, the data were described by the sum of six significant 2-D components. The parameters estimated by fitting are not shown, as they were essentially the same as the theoretical values in the upper part of Table 8. For this simulated data set, the mean error for estimates of the two open and three closed time constants was 0.34% (range 0.03–1.18%) and the mean error for the estimates of the volumes of the five components with volumes greater than zero was 1.2% (range 0.12–2.7%). For the sixth volume the fitted value was −0.0030 compared to the theoretical value of −0.0036.

Decreasing the number of simulated events to 100,000 increased the mean error in the time constants fitted to a single data set to 1.0% (range 0.1–1.8%) and increased the mean error in the five volumes greater than zero to 1.8% (range 0.2–5.5%). The estimated volume of the sixth component was −0.0021. Decreasing the number of simulated events further to 10,000 increased the mean error in the time constants fitted to a single data set to 2.1% (range 0.98–6.0%) and increased the average error in the five volumes greater than zero to 6.4% (range 0.3–14%). The estimated volume of the sixth component was −0.0055.

The 2-D components can be detected for a simple scheme consistent with gating of BK channels

As a further test of the ability to estimate the time constants and volumes of the components underlying 2-D dwell-time distributions, we simulated single-channel data for a simple kinetic model (Magleby and Pallotta, 1983) that has been used to describe the gating of a large conductance calcium-activated K channel, and compared the estimates of the fitted time constants and volumes to the theoretical values calculated from the model. The examined model, Scheme 5, has two open and three closed states and is often used for theoretical investigations of fitting methods (Blatz and Magleby, 1986; Crouzy and Sigworth, 1990; Fredkin and Rice, 1992; Magleby and Song, 1992; Qin et al., 1996). The theoretical 2-D components for Scheme 5 without filtering are shown in the upper part of Table 8.

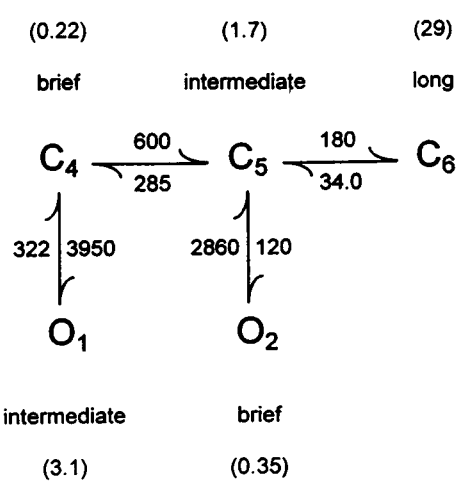

Scheme 5.

TABLE 8 Kinetic 2-D components for Scheme 5

τ_{open} (ms)		τ_{shut} (ms)		V_{Obs}	V_{Ind}	V_{Diff}	cDep
			Dead time = 0 ms				
O'_1	3.107	C'_4	0.218	0.7962	0.7449	0.0513	0.069
		C'_5	1.805	0.0990	0.1327	−0.0337	−0.254
		C'_6	44.763	0.0447	0.0622	−0.0176	−0.282
O'_2	0.350	C'_4	0.218	−0.0036	0.0476	−0.0513	−1.08
		C'_5	1.805	0.0422	0.0085	0.0337	3.97
		C'_6	44.763	0.0216	0.0040	0.0176	4.42
			Dead time = 0.15 ms				
O'_1	5.38	C'_4	0.23	0.790	0.739	0.051	0.069
		C'_5	1.93	0.098	0.130	−0.032	−0.247
		C'_6	46.6	0.050	0.069	−0.019	−0.272
O'_2	0.34	C'_4	0.23	−0.002	0.049	−0.051	−1.05
		C'_5	1.93	0.041	0.009	0.032	3.76
		C'_6	46.6	0.023	0.004	0.019	4.13

Decreasing the number of simulated events even further to 1000 still allowed the detection of the two open and three closed time constants giving six significant components ($p < 0.001$), but increased the average error in the time constants fitted to a single data set to 24% (range 3.2–42%), and increased the average error in the five volumes greater than zero to 19% (range 3.4–30%). The estimated volume of the sixth component was −0.0070.

When it is considered that the theoretical numbers of interval pairs (open-closed and closed-open) in the six components for Scheme 5 for 1000 simulated intervals were only about 796, 99, 45, −3.6, 42, and 22 (volumes in Table 8, upper part), the ability to both detect the components and estimate their parameters with mean errors that often appear to be less than those expected from stochastic variation alone appears to be nothing less than miraculous. However, the reason that the errors appear to be smaller than what might be expected from the limited numbers of events is that the 2-D fitting places internal constraints on parameter estimation. For example, it can be possible to determine the parameters defining a 2-D component with zero volume (no interval pairs) with fitting because the open and closed time constants defining the component are (individually) common to other components, and the volume can be determined by default, as all of the volumes must sum to 1.0 (Eqs. 4 and 5 and Appendix).

Testing for significance of the component dependencies

The practical interpretation of component dependencies determined from experimental data would require knowing whether their estimated values were significantly different from zero. A component dependency significantly different from zero would indicate an excess or deficit of interval pairs over that expected for independent pairing. The above section indicated that the analysis of 1000 simulated intervals was sufficient to detect the six expected components for Scheme 5. This section examines whether the component dependencies associated with the six detected components were significantly different from zero.

Resampling (Efron, 1982; Horn, 1987; Press et al., 1992) was used to estimate the potential variability in the estimates of component dependencies. The original 2-D distribution of 1000 pairs of adjacent open-shut intervals was sampled 1000 times to generate a artificial 2-D distribution with the same number of open-shut interval pairs as the original distribution. Some of the pairs of open-shut intervals from the original distribution would be included more than once in the artificial distribution and others would be missing. The artificial distribution was then fitted with sums of 2-D components, and the entire procedure was repeated 200 times to estimate the variability in the component dependencies of each of the six components.

Fig. 9 *A* plots a histogram of the 200 resampled estimates of the component dependency for component $O'_1C'_4$ from Scheme 5. The plot gives an approximate distribution of the estimates of the component dependencies that would be obtained assuming that the simulation and fitting were repeated 200 times. The arrow at 0.081 indicates the value estimated from the original distribution. The distribution deviated significantly from a Gaussian (smooth curve; $p < 0.01$, χ^2 test), as might be expected because the definition of component dependency involves a ratio (Eq. 6). Thus a nonparametric test of significance is indicated. The null hypothesis is that the component dependency is not significantly different from zero. Because a component dependency can be greater or less than zero, a two-tailed test was used. For a p value of 0.05, a component dependency would be significantly different from zero if less than 2.5% of the estimates ($0.025 \times 200 = 5$) are to one side of zero. Because none of the 200 resampled estimates in Fig. 9 *A* were less than zero, the null hypothesis can be rejected ($p \approx 0/200$). Applying the same nonparametric test to distributions for the other five components gave p values ranging from ~0 to 0.04. Thus all six component dependencies for Scheme 5 were significantly different from zero for the analysis of 1000 simulated intervals.

Repeating the entire analysis described above for 500 rather than 1000 simulated intervals gave the resampled distribution for component $O'_1C'_4$ shown in Fig. 9 *B*. The variability in the estimates was increased when fewer intervals were analyzed (compare to Fig. 9 *A*). The distribution in Fig. 9 *B* also deviated significantly from a Gaussian (smooth curve; $p < 0.01$, χ^2 test). Ten of the resampled estimates were to the left of zero, indicating that the component dependency of $O'_1C'_4$ was not significantly different from zero ($p \approx 0.1$). A similar analysis for the other five components indicated that none were significantly different from zero (p ranged from 0.1 to 0.46). Thus component dependencies significantly different from zero could be detected for Scheme 5 for 1000 analyzed intervals, but not for 500.

As a further examination of the adequacy of resampling to test for significance, the complete analysis described above was performed on 1000 simulated intervals for a

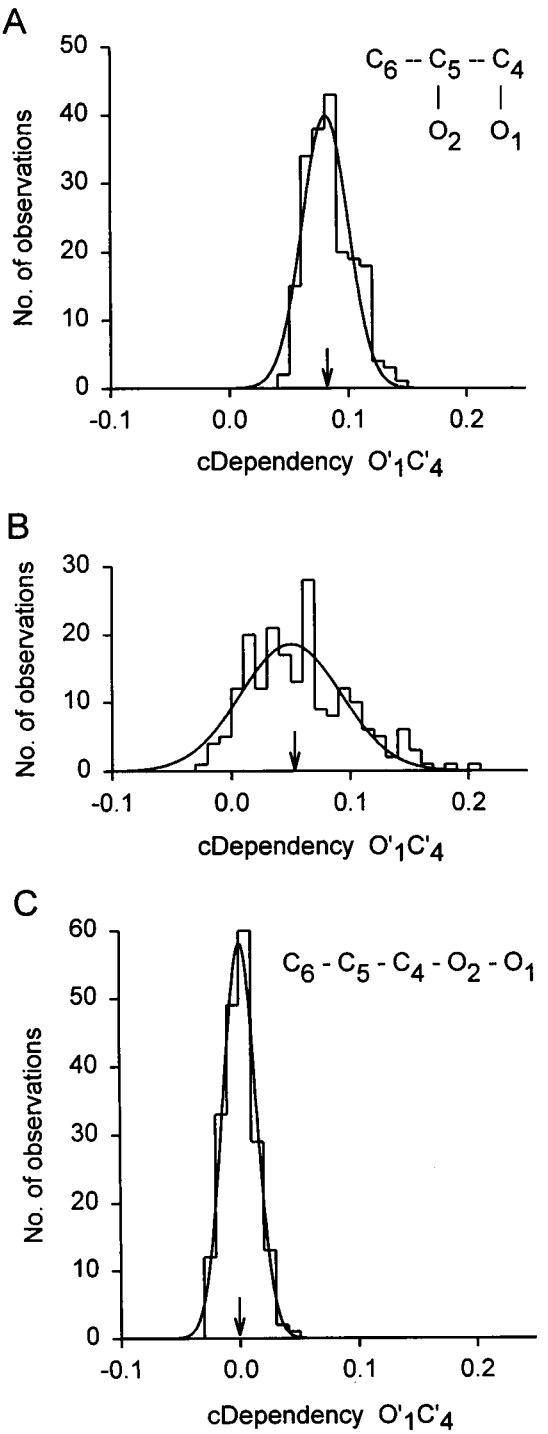

FIGURE 9 Estimating the significance of component dependencies with resampling. (*A* and *B*) Histogram of 200 estimates of the component dependency for component $O'_1C'_4$ from Scheme 5, obtained by resampling and refitting of the original 2-D distribution generated from 1000 simulated intervals for *A* and 500 simulated intervals for *B*. The arrows indicate the estimates of the component dependencies from the original distribution of 1000 intervals for *A* and 500 intervals for *B*. The smooth curves are Gaussian fits to the data. (*C*) Histogram of 200 estimates of the component dependency for component $O'_1C'_4$ obtained by resampling for a kinetic scheme with three closed and two open states and with a single gateway state (*inset*; same scheme and rate constants as Scheme 3 in Magleby and Song, 1992). The original 2-D distribution that was resampled was generated from 1000 simulated intervals.

kinetic scheme with three closed and two open states and a single gateway state (Fig. 9 *C*, *inset*). The expected component dependencies for a scheme with a single gateway state would be zero, as was the case for Scheme 2 (Table 4). The resampled distribution of component dependencies for component $O'_1C'_4$ is shown in Fig. 9 *C*. The distribution appeared to be centered about zero and did not deviate significantly from a Gaussian (smooth curve; $p > 0.5$, χ^2 test). Neither this component nor any of the other five components were significantly different from zero, consistent with a single gateway state.

The 2-D components can be detected in filtered and noisy data

Filtering and noise can distort experimental single-channel currents (Colquhoun and Sigworth, 1995). To investigate the effects of filtering and noise on the ability to estimate 2-D components by fitting 2-D dwell-time distributions with sums of 2-D components, a single-channel current record was simulated for Scheme 5 with true filtering to give a dead time of 0.15 ms and noise with a standard deviation of 15% of the single-channel amplitude (see Methods) and fitted with 2-D components. The fitted values of the volumes and time constants for 10^6 detected intervals (Table 8, lower part) were then compared to theoretical values (not shown) calculated with Q-matrix methods, assuming idealized filtering with a dead time of 0.15 ms (see Methods). The mean differences of the fitted parameters from the theoretical values describing the 2-D components were 2.1% (range 0.6–3.4%) for the time constants and 2.5% (range 0.6–4.1%) for five of the six volumes. The sixth volume was estimated by fitting as −0.0022 compared to a theoretical volume of −0.0040. For 10,000 detected events with true filtering and noise, the mean differences between the fitted and theoretical 2-D components were 4.2% (range 0.03–8.5%) for the time constants and 6.8% (range 0.36–11%) for five of the six volumes. The sixth volume was estimated as −0.011. For 1000 detected events with true filtering and noise, the mean differences between the fitted and theoretical 2-D components were 23% (range 3.4–42%) for the time constants and 36% (range 3.4–87%) for five of the six volumes. The sixth volume was estimated as −0.0071. The large variability for only 1000 fitted intervals is consistent with the stochastic variation expected for the limited numbers of intervals in most of the components.

The general agreement between the estimates obtained by fitting filtered simulated data and the estimates obtained by theoretical calculations from the kinetic scheme for filtered data suggest that the 2-D components can be estimated for Scheme 5 by fitting sums of 2-D components to 2-D dwell-time distributions with levels of true filtering and noise similar to those encountered in analysis of experimental data.

The correlation information can be retained when large numbers of intervals are undetected because of filtering

Fig. 10 presents component dependency plots for Scheme 5 obtained by simulating and fitting 10^6 intervals of single-channel data with various levels of filtering to give dead times of 0.0, 0.15, and 0.3 ms and noise in the filtered data with a standard deviation of 15% of the single-channel amplitude. For these dead times, it would be expected that 0%, 43%, and 65%, respectively, of the total intervals in the single-channel record would be not be detected because of filtering. Despite the large numbers of missed intervals, the directions and general magnitudes of the component dependencies determined from the data with filtering were similar to those in the absence of filtering (Fig. 9). Thus the correlation information could still be obtained from analysis of the single-channel data for Scheme 5 when large numbers of intervals were missed.

Potential detection of virtual components in heavily filtered single-channel data

The missed intervals that result from filtering can introduce potential virtual components in the dwell-time distributions. These virtual components have apparent time constants typically less than about half the dead time (Roux and Sauve, 1985; Magleby and Weiss, 1990a; Hawkes et al., 1992). Virtual components were not detected for the above example involving Scheme 5 when the dead time was 0.15 or 0.3 ms, provided that the fitting was started at twice the dead time. Fitting from the dead time resulted in a virtual shut component being detected for the data with a 0.3-ms dead time. Virtual components were detected for Scheme 5 when the dead time was 0.5 ms or greater, even when the fitting was started at twice the dead time.

Because it would not be clear for heavily filtered experimental data whether detected components with time constants less than about half the dead time arise from actual brief lifetime components or virtual components, the detection of virtual components and an assumption that they arise from real components could lead to an overestimation of the number of states when the dwell-time distributions are fitted directly with exponential components (see discussion in Colquhoun and Hawkes, 1995a). One test to distinguish between actual or virtual components would be to increase the filtering slightly. If the brief detected components were from virtual components, then increasing the filtering would make the brief components better defined with larger volumes, whereas if the brief detected components were actual, then increasing the filtering would have either little effect or make them less well defined.

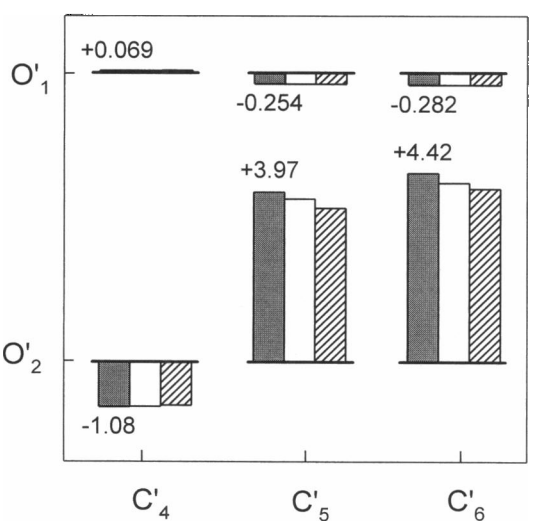

FIGURE 10 Component dependency plots for Scheme 5 with various levels of filtering and with noise in the single-channel data. The black bars are for data with no filtering (dead time of 0 ms) and no noise. The numerical values indicate the component dependencies for the black bars. The open and hatched bars are for fits of 2-D components to data simulated with filtering to give dead times of 0.15 ms and 0.3 ms, respectively. The filtered data had added noise with an amplitude equal to 15% of the single-channel current amplitude. Each analysis is based on 10^6 detected intervals.

DISCUSSION

This paper shows that component dependencies can give direct information about the gating mechanisms of ion channels and that the component dependencies can be estimated by fitting sums of 2-D (joint) exponential components to 2-D (joint) dwell-time distributions.

Applications of 2-D fitting

A typical step in the analysis of single-channel records often involves binning the open and shut interval durations into separate 1-D dwell-time distributions, which are then fitted with sums of exponentials to estimate the minimum number of open and closed states (Fig. 1 and Colquhoun and Sigworth, 1995). The results of our study suggest that it may be more advantageous to skip the 1-D analysis altogether and bin the data into 2-D dwell-time distributions, which are then fitted with sums of 2-D exponential components.

The fitting of 2-D distributions can, for some models, provide a more sensitive method of estimating the numbers of open and closed states. For Scheme 1 with three open and three closed states, the analysis of 2,000,000 open and shut intervals with 1-D fitting was not sufficient to detect the third open state. Yet the analysis of 50,000 open and shut intervals with 2-D fitting allowed the detection of the third open state (Table 7).

After the numbers of open and closed states have been estimated with 2-D fitting, calculation of component dependencies (Eqs. 6–8) from the fitted 2-D components can provide further insight into gating mechanisms. The technique is especially useful, because the information provided by the component dependencies does not require an a priori

assumption of a kinetic scheme. Classes of models that appear consistent with the component dependencies can serve as starting points for developing gating mechanisms, and classes of models that are inconsistent with the component dependencies can be excluded.

The powerful maximum likelihood methods typically used to develop gating mechanisms provide a quantitative means of ranking the examined models by likelihood (Horn and Lange, 1983; Ball and Sansom, 1989; Magleby and Weiss, 1990b; Chung et al., 1991; Fredkin and Rice, 1992; Qin et al., 1996; Colquhoun et al., 1996). However, they do not provide a systematic means of examining whether the top ranked model actually accounts for the detailed features of the gating. Because there is no guarantee that the "correct" model has been examined or even that channels gate in the simple manner portrayed by typical models, there needs to be additional ways of examining the proposed gating mechanisms. The component dependencies can provide one such approach. A systematic comparison of each of the component dependencies predicted by the top-ranked kinetic scheme to those obtained by fitting 2-D components directly to experimental data should immediately indicate whether the top-ranked kinetic scheme captures all of the basic features of the gating. If not, then the differences between the predicted and observed component dependencies should give insight into where the kinetic scheme needs modification.

Application of 2-D fitting can also provide a guide to whether the most likely model has actually been found by the various analysis procedures. If the maximum likelihood value for fitting the experimental 2-D dwell-time distribution with sums of 2-D components, where the free parameters are the time constants and volumes, is the same as the likelihood value for fitting the experimental 2-D dwell-time distribution with a specific kinetic scheme, where the free parameters are the rate constants, then this would suggest that no other model with the same number of states will be found that can give a better description of the data. Such an observation does not exclude the possibility that additional gating mechanisms with the same number of states may be found that are equally likely. Methods for fitting rate constants to kinetic schemes using 2-D dwell-time distributions were not considered in this paper, because they have been described previously (Magleby and Weiss, 1990b; Rothberg et al., 1997).

2-D fitting does not require binning of the data

The analysis carried out in this paper does not require that the pairs of adjacent open and shut intervals be binned into 2-D distributions. The interval pairs could be fitted directly by calculating the likelihood for each pair of intervals rather than the likelihood of each bin of paired intervals. For fewer than about 1000 interval pairs, fitting the paired intervals rather than the binned paired intervals to obtain estimates of the 2-D components may be faster. However, for large numbers of interval pairs, fitting binned data can be orders of magnitude faster. If probabilities are based on the volumes of the bins rather than their magnitudes, as described in the Appendix (Eq. A4), and if there is a minimum of 10 bins per log unit, then any errors introduced by fitting binned data should be negligible. Binning has the advantage that it presents a method for graphical display of the data through plotted 2-D distributions.

Limitations of 2-D fitting

The theory (Fredkin et al., 1985) underlying the fitting of 2-D dwell-time distributions with sums of 2-D components (Eq. 4) was based on an assumption of discrete-state Markov gating. Thus the practical application of decomposing 2-D dwell-time distributions into 2-D exponential components will be limited to those channels that gate by making transitions among a discrete number of states with rate constants for transitions among the states remaining constant in time for constant experimental conditions. ACh receptor channels (Colquhoun and Sakmann, 1985), Na^+ channels (Hahin, 1988), fast Cl^- channels (Blatz and Magleby, 1989), GABA receptors (Weiss and Magleby, 1989), native BK channels (McManus and Magleby, 1989; Petracchi et al., 1991), and *N*-methyl-D-aspartate receptors (Gibb and Colquhoun, 1992) have burst patterns and time constants of conditional distributions that appear independent of previous activity, suggesting Markov gating. Thus the methods described in this paper may be applicable to these channels.

If all of the component dependencies derived from a 2-D dwell-time distribution are zero, then such an observation would suggest that there is a single gateway state and that the component dependencies contain no additional information about the connections among states. Nevertheless, the analysis of 2-D distributions will always give more kinetic information than analysis of 1-D distributions, because the observation of component dependencies of zero excludes models with more than one gateway state. Some simple examples were presented to show how component dependencies can be used to suggest kinetic gating mechanisms. However, models suggested by component dependencies are not necessarily unique, as models with different gating mechanisms can display identical single-channel kinetics (Fredkin et al., 1985; Bauer et al., 1987; Kienker, 1989). Thus component dependencies can be used only to suggest classes of models, but not unique models.

For models with many states and models with fast transitions among the states, it can be difficult to interpret the component dependencies in terms of possible mechanisms, as the components generated by such models can be counterintuitive, with no obvious relationship between components and states. For the simple models examined in our study, the states or compound states underlying the components with the greatest component dependencies were directly connected, and the states or compound states under-

lying the components with component dependencies less than or equal to -1.0 were not effectively connected, because of intervening states of longer lifetimes. Although there may be exceptions to these observations for some gating mechanisms, the observations can serve as a starting point for interpreting component dependency plots. Further study of models and their predicted component dependencies should provide additional information toward interpretation.

The 2-D analysis presented in this study requires that the gating of the channel be in a steady state during the collection of data. Therefore the 2-D method could be used to analyze data obtained at, for example, two different agonist concentrations, but it could not be used to analyze data obtained during a change in agonist concentration. The 2-D analysis, as presented, is not applicable to the analysis of channels that spend significant amounts of time in subconductance states. Thus for nonstationary data or data containing appreciable subconductance levels, an estimate of the correlation information may best be obtained indirectly from the most likely kinetic scheme fitted by the full likelihood approach (Horn and Lange, 1983; Ball and Sansom, 1989; Chung et al., 1991; Fredkin and Rice, 1992; Qin et al., 1996; Colquhoun et al., 1996).

As is the case for all analysis methods, the number of intervals needed to define the various components will depend on the volumes and time constants of the components. For example, 50,000 intervals were required to detect all nine 2-D components describing data from Scheme 1, whereas only 1000 intervals were needed to detect the six 2-D components describing data from Scheme 5 (see Results: Part 2). Thus a limitation of the 2-D method (and all methods of analysis) is that the number of intervals analyzed may be less than required to define the complexities of the gating, leading to simplified models. For small data sets of a few hundred intervals, the full likelihood approach may best be used to extract any available correlation information, because the correlation information may not be significant in the component dependencies, but could be reflected in the likelihood values.

Extension of the analysis

The focus of this paper has been restricted to 2-D distributions of adjacent open and shut intervals. However, for gating mechanisms with two or more gateway states in which the time constants of the open components are identical, analysis of open-shut distributions would indicate a single open component and component dependencies of zero, suggesting incorrectly that there was a single transition pathway between open and closed states. To overcome this limitation, the 2-D dwell-time distribution of the durations of pairs of consecutive shut intervals (those separated by a single open interval) could be analyzed (examples of shut-shut distributions appear in Song and Magleby, 1994). If the shut-shut component dependencies differed significantly from zero, then this would indicate that there are two or more gateway states. Thus the shut-shut component dependencies could give additional information about the connections among states. Alternatively, if the shut components all had identical time constants but the open components did not, then the 2-D distributions of pairs of consecutive open intervals could be analyzed to obtain correlation information not contained in the open-shut distributions.

When microscopic reversibility is obeyed, the 2-D distributions of adjacent open and shut intervals obtained from analyzing the single-channel current record in either the forward or backward direction (in time) should be indistinguishable (Fredkin et al., 1985; Steinberg, 1987b). Comparison of forward and backward distributions by Song and Magleby (1994) indicated no significant differences for the gating of the BK channel. It is possible that comparisons of the 2-D components and component dependencies for forward and backward analysis of the data could provide a more sensitive test for microscopic reversibility, as differences might be detected in the underlying components that would be averaged out when the entire 2-D distributions are compared.

CONCLUSION

Although it has been known since the pioneering work of Fredkin et al. (1985) that the 2-D dwell-time distributions of adjacent open and shut intervals are composed of the sums of 2-D exponential components, the present study is the first to examine whether the underlying 2-D components predicted by the theory can be determined directly by fitting. Our findings suggest that the components can be determined directly and that their transformation into component dependencies can then give direct insight into possible gating mechanisms.

APPENDIX: FITTING 2-D DWELL-TIME DISTRIBUTIONS WITH SUMS OF 2-D EXPONENTIAL COMPONENTS

A 2-D dwell-time distribution generated by a discrete-state Markov model is composed of the sums of $N_O \times N_C$ 2-D components, where N_O and N_C are the numbers of open and closed states (Fredkin et al., 1985, and Eq. 4). This section details how the 2-D components and the numbers of open and closed states can be estimated by maximum likelihood fitting of 2-D dwell-time distributions. The approach is an extension of the 1-D method presented by Colquhoun and Sigworth (1995), except that 2-D (joint) probabilities are used.

The exponential composition of 1-D and 2-D dwell-time distributions generated by Markov models are described by Eqs. 2–5 in the Theory section of this paper, which should be read before proceeding with this section. The (joint) probability $f_{OC}(t_O, t_C)$ of observing an open-closed interval pair consisting of an open interval of duration t_O followed by a closed interval of duration t_C is proportional to

$$f_{OC}(t_O, t_C) = \sum_{i=1}^{N_O} \sum_{j=1}^{N_C} V_{ij}\tau_i^{-1}\tau_j^{-1}\exp(-t_O/\tau_i)\exp(-t_C/\tau_j) \quad \text{(A1)}$$

where N_O and N_C are the number of open and closed states, V_{ij} is the volume of each 2-D component (fraction of total open-closed interval

pairs), and τ_i and τ_j are the time constants of the open and closed exponential functions. The magnitude of each individual 2-D component (at zero time) is given by $V_{ij}\tau_i^{-1}\tau_j^{-1}$. The volumes of the $N_O \times N_C$ underlying components sum to 1.0.

Equation A1 describes the probability density for $t = 0$ to infinity. In practice, the limited time resolution of single-channel currents imposes a lower limit on the duration of the briefest detected interval, t_{low}. An upper limit, t_{high}, may also be imposed to truncate the fitted distribution, because it may occasionally be advantageous to exclude from the data long closed intervals, such as those resulting from slow blocks or inactivated states. For a 2-D distribution the probability $P(t_{low} < t < t_{high})$ that the durations of both intervals in an open-closed interval pair fall between t_{low} and t_{high} is given by

$$P(t_{low} < t < t_{high}) = \sum_{i=1}^{N_O}\sum_{j=1}^{N_C} V_{ij}[\exp(-t_{low}/\tau_i) - \exp(-t_{high}/\tau_i)][\exp(-t_{low}/\tau_j) - \exp(-t_{high}/\tau_j)] \quad (A2)$$

Thus the probability of observing a open-shut interval pair from a population in which both intervals in each pair have durations between t_{low} and t_{high} is proportional to

$$f_{OC}(t_O, t_C | t_{low} < t < t_{high}) = \frac{f_{OC}(t_O, t_C)}{P(t_{low} < t < t_{high})} \quad (A3)$$

To greatly reduce the amount of time required for fitting, interval pairs can be log-binned (McManus et al., 1987; Sigworth and Sine, 1987), and likelihoods calculated using bin volumes. The probability $V_{bin}(t_1, t_2, t_3, t_4)$ of observing an interval pair in a 2-D bin is given by

$$V_{bin}(t_1, t_2, t_3, t_4) = \sum_{i=1}^{N_O}\sum_{j=1}^{N_C} V_{ij}[\exp(-t_1/\tau_i) - \exp(-t_2/\tau_i)] \cdot [\exp(-t_3/\tau_j) - \exp(-t_4/\tau_j)] \quad (A4)$$

where t_1 and t_2 are the beginning and ending times for the open dimension of a given 2-D bin and t_3 and t_4 are the beginning and ending times for the closed dimension of the same bin.

The log-likelihood $L(\theta)$ is then calculated as

$$L(\theta) = \sum_{j=1}^{N_{bin}} n_j \log_e \frac{V_{binj}(t_1, t_2, t_3, t_4)}{P(t_{low} < t < t_{high})} \quad (A5)$$

where N_{bin} is the number of bins, n_j is the number of observations in bin j, and $\log_e$ is the natural logarithm. Using bin volumes to calculate the likelihood avoids binning errors that can be introduced if bin midtimes are used (McManus et al., 1987). In practice, computing time can be reduced by replacing Eq. A5 with

$$L(\theta) = \left[\sum_{j=1}^{N_{bin}} n_j \log_e V_{binj}(t_1, t_2, t_3, t_4)\right] - [n_{total} \log_e P(t_{low} < t < t_{high})] \quad (A6)$$

where n_{total} is the total number of fitted open-closed interval pairs. This allows the division of the bin volumes by the denominator to be replaced by a single operation at the end of the likelihood calculation.

The free parameters optimized in the likelihood fitting are the time constants of the N_O open and N_C closed exponential functions, the product of which generates the $N_O \times N_C$ 2-D components, and the volumes of the 2-D components. However, because the volumes must sum to 1.0, one of the volumes is considered to be constrained (not free). Thus the number of free parameters N_{free} required to describe the 2-D components that sum to generate a 2-D dwell-time distribution is given by

$$N_{free} = N_O + N_C + (N_O \times N_C) - 1 \quad (A7)$$

Table 9 indicates the number of free parameters for various numbers of open and closed exponential functions underlying the 2-D distribution.

The number of significant open and closed exponential functions was determined with the likelihood ratio test, in which twice the log of the likelihood ratio is distributed as χ^2 (Rao, 1973; Horn and Lange, 1983). Each 2-D distribution was fitted with an increasing number of 2-D components by increasing the numbers of open and closed time constants, and the fits were then compared by determining $\log_e R_k$ from

$$\log_e R_k = \log_e(L_k/L_{k-1}) = \log_e L_k - \log_e L_{k-1} \quad (A8)$$

where $\log_e R_k$ is the natural logarithm of the likelihood ratio of the two different 2-D distributions described by k versus $k - 1$ time constants, and L_k and L_{k-1} are the likelihoods that the data were drawn from the two different fitted 2-D distributions.

To determine whether any increase in likelihood resulting from an additional time constant was significant, $\log_e R_k$ from Eq. A8 was multiplied by 2.0, and the p value was determined from a χ^2 table. The degrees of freedom used with the χ^2 table were determined from Table 9 as the difference in the number of free parameters before and after fitting with an additional time constant. For example, a 2-D distribution described by four closed exponential functions, two open exponential functions, and eight volumes of the 2-D components ($4 + 2 + (4 \times 2) - 1 = 13$ free parameters) would give a significantly better description of the data ($p \leq 0.05$) compared to three closed exponential functions, two open exponential functions, and six volumes (10 free parameters) if the likelihood ratio were ≥ 3.907, because the χ^2 value at $p = 0.05$ for three degrees of freedom is 7.815. Table 10 indicates the minimum log-likelihood ratios $\log_e R_k$ required for the statistical significance of an additional component for the indicated degrees of freedom. The values in the table were calculated by first computing a χ^2 table (Press et al., 1992) and then dividing the χ^2 values by 2.

When fitting, open and closed time constants are added one at a time until the likelihood is no longer improved significantly by an additional time constant. An estimate of the minimum number of open and closed states is then given by the number of significant open and closed time constants, respectively, underlying the fit to the 2-D distribution.

For the various kinetic gating mechanisms examined in this paper, the 2-D fitting method appeared relatively insensitive to the starting parameters. The most likely time constants and volumes were typically found with a single set of starting parameters. In practice, the fits were repeated several times with different sets of starting parameters to increase the probability of finding the most likely fit. The fitting routine used a simple univariate search algorithm in which the values of the parameters were changed one at a time and the step size for each parameter was autoranging.

The distribution of brief intervals can be distorted due to the narrowing of brief events by filtering (McManus et al., 1987; Colquhoun and Sigworth, 1995). Errors in parameter estimation that can result from this

TABLE 9 Number of free parameters when fitting 2-D dwell-time distributions with sums of 2-D components

No. of shut time constants	No. of open time constants				
	1	2	3	4	5
1	2	4	6	8	10
2	4	7	10	13	16
3	6	10	14	18	22
4	8	13	18	23	28
5	10	16	22	28	34
6	12	19	26	33	40
7	14	22	30	38	46
8	16	25	34	43	52

TABLE 10 Minimum difference between log-likelihoods required for significance with the indicated number of additional free parameters

Additional free parameters	p values		
	0.05	0.01	0.001
2	2.996	4.605	6.908
3	3.907	5.672	8.133
4	4.744	6.638	9.233
5	5.535	7.543	10.258
6	6.296	8.406	11.229
7	7.034	9.238	12.161
8	7.754	10.045	13.062
9	8.460	10.833	13.939

The tabulated values are computed χ^2 values divided by 2.

distortion can be minimized by either 1) setting t_{low} to twice the system deadtime (t_{dead}), which would exclude the narrowed intervals from the fit, or 2) correcting the brief interval durations to their estimated true durations (Colquhoun and Sigworth, 1995). When fitting 2-D distributions, it may be preferable to correct the brief interval durations, as eliminating all pairs of intervals in which one or both of the intervals have a duration of less than $2 \times t_{dead}$ can result in a significant loss of data. However, correcting and fitting intervals with durations of less than $2 \times t_{dead}$ can introduce error, because with some gating mechanisms and levels of filtering, intervals less than the dead time can be detected (see Magleby and Weiss, 1990a, Fig. 3), placing an excess of intervals in the first few bins.

The missed events that result from filtering can introduce extra components with time constants typically less than one-half the dead time (Roux and Sauve, 1985; Hawkes et al., 1992; Magleby and Weiss, 1990a). Fitting from $2 \times t_{dead}$ will typically exclude the detection of the virtual components if the filtering is not excessive (see Methods and Results).

This work was supported in part by grants from the National Institutes of Health (AR32805, NS30584, NS007044) and the Muscular Dystrophy Association.

REFERENCES

Aldrich, R. W., D. P. Corey, and C. F. Stevens. 1983. A reinterpretation of mammalian sodium channel gating based on single channel recording. *Nature.* 306:436–441.

Auerbach, A. 1993. A statistical analysis of acetylcholine receptor activation in *Xenopus* myocytes: stepwise versus concerted models of gating. *J. Physiol. (Lond.).* 461:339–378.

Ball, F. G., C. J. Kerry, R. L. Ramsey, M. S. Sansom, and P. N. Usherwood. 1988. The use of dwell time cross-correlation functions to study single-ion channel gating kinetics. *Biophys. J.* 54:309–320.

Ball, F. G., and M. S. Sansom. 1989. Ion-channel gating mechanisms: model identification and parameter estimation from single channel recordings. *Proc. R. Soc. Lond. Biol.* 236:385–416.

Bauer, R. J., B. F. Bowman, and J. L. Kenyon. 1987. Theory of the kinetic analysis of patch-clamp data. *Biophys. J.* 52:961–978.

Bezanilla, F., E. Perozo, and E. Stefani. 1994. Gating of Shaker K^+ channels. II. The components of gating currents and a model of channel activation. *Biophys. J.* 66:1011–1021.

Blatz, A. L., and K. L. Magleby. 1986. Correcting single channel data for missed events. *Biophys. J.* 49:967–980.

Blatz, A. L., and K. L. Magleby. 1989. Adjacent interval analysis distinguishes among gating mechanisms for the fast chloride channel from rat skeletal muscle. *J. Physiol. (Lond.).* 410:561–585.

Chung, S. H., V. Krishnamurthy, and J. B. Moore. 1991. Adaptive processing techniques based on hidden Markov models for characterizing very small channel currents buried in noise and deterministic interferences. *Philos. Trans. R. Soc. Lond. Biol.* 334:357–384.

Colquhoun, D., and A. G. Hawkes. 1981. On the stochastic properties of single ion channels. *Proc. R. Soc. Lond. Biol.* 211:205–235.

Colquhoun, D., and A. G. Hawkes. 1987. A note on correlations in single ion channel records. *Proc. R. Soc. Lond. Biol.* 230:15–52.

Colquhoun, D., and A. G. Hawkes. 1995a. The principles of the stochastic interpretation of ion-channel mechanisms. *In* Single-Channel Recording. B. Sakmann and E. Neher, editors. Plenum Press, New York. 397–482.

Colquhoun, D., and A. G. Hawkes. 1995b. A Q-matrix cookbook. *In* Single-Channel Recording. B. Sakmann and E. Neher, editors. Plenum Press, New York. 589–633.

Colquhoun, D., A. G. Hawkes, and K. Srodzinski. 1996. Joint distributions of apparent open times and shut times of single ion channels and maximum likelihood fitting of mechanisms. *Philos. Trans. R. Soc. Lond. A.* 354:2555–2590.

Colquhoun, D., and B. Sakmann. 1985. Fast events in single-channel currents activated by acetylcholine and its analogues at the frog muscle end-plate. *J. Physiol. (Lond.).* 369:501–557.

Colquhoun, D., and F. J. Sigworth. 1995. Fitting and statistical analysis of single-channel records. *In* Single-Channel Recording. B. Sakmann and E. Neher, editors. Plenum Press, New York. 483–587.

Crouzy, S. C., and F. J. Sigworth. 1990. Yet another approach to the dwell-time omission problem of single-channel analysis. *Biophys. J.* 58:731–743.

Efron, B. 1982. *The Jacknife, the Bootstrap, and Other Resampling Plans.* Society for Industrial and Applied Mathematics, Philadelphia.

Fredkin, D. R., M. Montal, and J. A. Rice. 1985. Identification of aggregated Markovian models: application to the nicotinic acetylcholine receptor. *In* Proceedings of the Berkeley Conference in Honor of Jerzy Neyman and Jack Kiefer. L. M. LeCam and R. A. Olshen, editors. Wadsworth Press, Belmont, CA. 269–289.

Fredkin, D. R., and J. A. Rice. 1992. Maximum likelihood estimation and identification directly from single-channel recordings. *Proc. R. Soc. Lond. Biol.* 249:125–132.

Gibb, A. J., and D. Colquhoun. 1992. Activation of NMDA receptors by L-glutamate in cells dissociated from adult rat hippocampus. *J. Physiol. (Lond.).* 456:143–179.

Hahin, R. 1988. Removal of inactivation causes time-invariant sodium current decays. *J. Gen. Physiol.* 92:331–350.

Hawkes, A. G., A. Jalali, and D. Colquhoun. 1992. Asymptotic distributions of apparent open times and shut times in a single channel record allowing for the omission of brief events. *Philos. Trans. R. Soc. Lond. Biol.* 337:383–404.

Hille, B. 1995. Ionic Channels of Excitable Membranes. Sinauer Associates, Sunderland, MA.

Horn, R. 1987. Statistical methods for model discrimination: application to gating kinetics and permeation of the acetylcholine receptor channel. *Biophys. J.* 51:255–263.

Horn, R., and K. Lange. 1983. Estimating kinetic constants from single channel data. *Biophys. J.* 43:207–223.

Jackson, M. B., B. S. Wong, C. E. Morris, H. Lecar, and C. N. Christian. 1983. Successive openings of the same acetylcholine receptor channel are correlated in open time. *Biophys. J.* 42:109–114.

Kienker, P. 1989. Equivalence of aggregated Markov models of ion-channel gating. *Proc. R. Soc. Lond. Biol.* 236:269–309.

Magleby, K. L., R. A. Bello, and B. S. Rothberg. 1997. Hidden components and hidden dependencies determined from two-dimensional (2-D) distributions from single BK channels in rat skeletal muscle. *Biophys. J.* 72:A130.

Magleby, K. L., and B. S. Pallotta. 1983. Calcium dependence of open and shut interval distributions from calcium-activated potassium channels in cultured rat muscle. *J. Physiol. (Lond.).* 344:585–604.

Magleby, K. L., and L. Song. 1992. Dependency plots suggest the kinetic structure of ion channels. *Proc. R. Soc. Lond. Biol.* 249:133–142.

Magleby, K. L., and D. S. Weiss. 1990a. Estimating kinetic parameters for single channels with simulation. A general method that resolves the missed event problem and accounts for noise. *Biophys. J.* 58:1411–1426.

Magleby, K. L., and D. S. Weiss. 1990b. Identifying kinetic gating mechanisms for ion channels by using two-dimensional distributions of simulated dwell times. *Proc. R. Soc. Lond. Biol.* 241:220–228.

McManus, O. B., A. L. Blatz, and K. L. Magleby. 1985. Inverse relationship of the durations of adjacent open and shut intervals for Cl and K channels. *Nature.* 317:625–627.

McManus, O. B., A. L. Blatz, and K. L. Magleby. 1987. Sampling, log binning, fitting, and plotting durations of open and shut intervals from single channels and the effects of noise. *Pflugers Arch. Eur. J. Physiol.* 410:530–553.

McManus, O. B., and K. L. Magleby. 1988. Kinetic states and modes of single large-conductance calcium-activated potassium channels in cultured rat skeletal muscle. *J. Physiol. (Lond.).* 402:79–120.

McManus, O. B., and K. L. Magleby. 1989. Kinetic time constants independent of previous single-channel activity suggest Markov gating for a large conductance Ca-activated K channel. *J. Gen. Physiol.* 94: 1037–1070.

McManus, O. B., and K. L. Magleby. 1991. Accounting for the Ca^{2+}-dependent kinetics of single large-conductance Ca^{2+}-activated K^+ channels in rat skeletal muscle. *J. Physiol. (Lond.).* 443:739–777.

Neher, E., and C. F. Stevens. 1977. Conductance fluctuations and ionic pores in membranes. *Annu. Rev. Biophys. Bioeng.* 6:345–381.

Petracchi, D., M. Barbi, M. Pellegrini, M. Pellegrino, and A. Simoni. 1991. Use of conditioned distributions in the analysis of ion channel recordings. *Eur. Biophys. J.* 20:31–39.

Press, W. H., S. A. Teukolsky, W. T. Vetterling, and B. P. Flannery. 1992. Numerical Recipies in C. Cambridge University Press, Cambridge, England.

Qin, F., A. Auerbach, and F. Sachs. 1996. Estimating single-channel kinetic parameters from idealized patch-clamp data containing missed events. *Biophys. J.* 70:264–280.

Rao, C. R. 1973. Linear Statistical Inference and Its Applications. John Wiley and Sons, New York.

Rothberg, B. S., R. A. Bello, and K. L. Magleby. 1997. Gating mechanisms for single BK channels determined using Q-matrix fitting of two-dimensional dwell-time distributions. *Biophys. J.* 72:A130.

Roux, B., and R. Sauve. 1985. A general solution to the time interval omission problem applied to single channel analysis. *Biophys. J.* 48: 149–158.

Sigworth, F. J., and S. M. Sine. 1987. Data transformations for improved display and fitting of single-channel dwell time histograms. *Biophys. J.* 52:1047–1054.

Sine, S. M., T. Claudio, and F. J. Sigworth. 1990. Activation of *Torpedo* acetylcholine receptors expressed in mouse fibroblasts. *J. Gen. Physiol.* 96:395–437.

Song, L., and K. L. Magleby. 1994. Testing for microscopic reversibility in the gating of maxi K^+ channels using two-dimensional dwell-time distributions. *Biophys. J.* 67:91–104.

Steinberg, I. Z. 1987a. Frequencies of paired open-closed durations of ion channels. Method of evaluation from single-channel recordings. *Biophys. J.* 52:47–55.

Steinberg, I. Z. 1987b. Relationship between statistical properties of single ionic channel recordings and the thermodynamic state of the channels. *J. Theor. Biol.* 124:71–87.

Weiss, D. S., and K. L. Magleby. 1989. Gating scheme for single GABA-activated Cl channels determined from stability plots, dwell-time distributions, and adjacent-interval durations. *J. Neurosci.* 9:1314–1324.

Zagotta, W. N., T. Hoshi, and R. W. Aldrich. 1994. Shaker potassium channel gating. III. Evaluation of kinetic models for activation. *J. Gen. Physiol.* 103:321–362.